U.PORTO

FEUP FACULDADE DE ENGENHARIA
UNIVERSIDADE DO PORTO

IMPACT OF ADHESIVE JOINTS FOR THE AUTOMOTIVE INDUSTRY AT LOW AND HIGH TEMPERATURES

SUBMITTED BY

Rodrigo Avendaño Mata

SUPERVISED BY

Lucas Filipe Martins da Silva

CO-SUPERVISED BY

Guilherme Viana and Marcelo Costa

JULY 2014

Abstract

In recent years there has been an increasing interest in the automotive industry in applying adhesive bonding in structural components of vehicles. Toughened, high performance adhesives can provide exceptional strength while producing lighter structures and, therefore, improve vehicle safety and efficiency. When adhesive joints are used in this area, some factors such as impact loading and temperature variation have a decisive role. Under these conditions, the joint must provide enough strength to transmit the load without fracturing, and thus assure the car's integrity. Although several studies have characterized adhesives under both situations separately, very few have considered them at the same time.

The objective of this study was to characterize the impact strength of a new crash resistant epoxy adhesive as a function of temperature. To achieve this, single lap joints specimens with ductile adherends were tested under drop weight impact at -20, +23 and +80 ºC, in order to emulate real situations. Induction heating and nitrogen gas cooling systems were designed and implemented to reach homogeneously the high and low temperatures in the overlap.

Then, properties of steel were obtained by conducting tensile tests. Bulk adhesive specimens were also tested at high and room temperatures in order to understand the influence of temperature on the adhesive properties.

Finally, the results were discussed and analyzed, and a failure prediction was developed. As a result, at room temperature failure was mostly dictated by the adherends yielding due to the high strength of the adhesive. At high and low temperatures, it was found a high decrease in the adhesive strength with an increase of ductility and brittleness, respectively. Thus, in this case it was the adhesive which determined the joints strength. Furthermore, although at room temperature the adherend yielding model gave accurate prediction, at high temperature the values predicted using the static properties of the adhesive were below the experimental due to the adhesive sensitiviy to the high strain-rate.

Resumen

Recientemente un creciente interés ha surgido en la industria del automóvil utilizar la unión adhesiva en los componentes estructurales de los vehículos. Los adhesivos endurecidos de alto rendimiento pueden proveer una excepcional resistencia y aligerar estructuras al mismo tiempo y, con ello, mejorar la seguridad y eficiencia del vehículo. Cuando se usan juntas adhesivas en este campo, algunos factores como el impacto o la variación de temperatura interpretan un papel decisivo. Bajo estas condiciones, la junta debe resistir lo suficiente para transmitir la carga sin fracturar, asegurando así la integridad del coche. A pesar de la existencia de diversos estudios que caracterizan adhesivos sometidos a estas situaciones separadamente, muy pocos las han considerado al mismo tiempo.

El objetivo de este estudio consiste en caracterizar la resistencia al impacto en función de la temperatura de un adhesivo epoxi nuevo y resistente al choque. Para ello, juntas SLJs con adherentes dúctiles fueron testeadas bajo impacto a -20, +23 y +80 ºC, simulando una situación real. Unos sistemas de calentamiento por inducción y enfriamiento mediante gas nitrógeno fueron diseñados e implementados para alcanzar dichas temperaturas durante el testeo.

Seguidamente, el acero usado para los adherentes fue testeado a tracción para determinar sus propiedades y, en el caso del adhesivo, estos tests se realizaron a +23 y +80 ºC, con el objetivo de estudiar la influencia de la temperatura en sus propiedades. Para acabar se llevó a cabo un análisis de los resultados y un modelo de predicción de fallida fue desarrollado.

Como resultado, a temperatura ambiente el fallo fue dictado por la deformación plástica de los adherentes debido a la gran resistencia del adhesivo. A altas y bajas temperaturas, en cambio, hubo una gran disminución en la fuerza del adhesivo, juntamente con un aumento de la ductilidad y la fragilidad, respectivamente. Por ello, en este caso fue el adhesivo el que determinó la resistencia de la junta. Aunque a temperatura ambiente el modelo de predicción por deformación de los adherentes resultó ser bastante preciso, a altas temperaturas la predicción mediante las propiedades estáticas del adhesivo dio valores inferiores a los experimentales, debido a la sensibilidad de éste a las grandes velocidades de deformación.

Acknowledgments

I would like to thank:

- Prof. Lucas Filipe Martins da Silva, for putting his trust on me for the presented work, guiding me with his supervision and encouraging me to do my best.
- Eng. Guilherme Viana and Marcelo Costa, for their invaluable help and patience, and for the many hours spent in their company.
- All the Adhesives Group of FEUP, especially Ricardo and Eduardo, for their essential contribution and advice.
- Mr. Miguel Figueiredo from the *Laboratório de Ensaios Tecnólogicos* for his help while performing the impact tests.
- My home faculty ETSEIB (UPC) for giving me the opportunity to enjoy this international learning, and FEUP for their warm welcome and hospitality.
- My friends for their endless support, especially Luis and Cristina, who have been always by my side during this experience.
- My family, for allowing me make them feel proud, and for making this possible.

Contents

List of Figures

List of tables

List of acronyms and symbols

Acronyms

SLJ	Single lap joints
FEA	Finite element analysis
RT	Room temperature
CTE	Coefficients of thermal expansion

Symbols

b	Joint Width	V	Transverse Force
l	Overlap Length	k	Bending Moment Factor
c	Half of Overlap Length	k'	Transverse Force Factor
t	Adherend Thickness	τ	Shear stress
t_t	Top Adherend Thickness	σ	Tensile stress
t_b	Bottom Adherend Thickness	ε	Strain
t_a	Adhesive Thickness	E	Adherend Young's Modulus
P	Applied Load	E_a	Adhesive Young's Modulus
$\bar{P}$	Applied Load per Unit Width	G_a	Adhesive Shear Modulus
M	Bending Moment	D	Adherend Bending Stiffness

1. Introduction

1.1 Background and motivation

In recent years the use of adhesive bonding for the automotive industry has become one of the cornerstones in the design of lighter structures. An essential factor to consider when joining by structural adhesive different parts of a vehicle is the resistance under impact load. Epoxy adhesives are commonly used in this kind of situations due to their high strength. In spite of the brittleness of pure epoxy resins, recent technological advances have improved toughness without reducing too much the joint strength by the addition of rubber particles.

Nowadays more attention is given in studies under impact phenomena where other environmental conditions are considered at the same time, with the aim of assuring the transfer of the load to the steel without fracturing the joint. Variation of the temperature while joints undergo to impact loads is one of the most relevant factors to study by experimental testing, since their behaviour under high strain-rate can be highly sensitive to temperature.

1.2 Objectives

The main objective of this thesis is to characterize a new developed epoxy adhesive under impact load at different temperatures. The adhesive studied is a new crash resistant version that combines properties of an epoxy adhesive and typical polyurethane adhesive, giving high strength, elongation and toughness. The adhesive joints were tested under impact load at a range of temperatures between -20 ºC and +80 ºC, in order to accurately emulate the real situation.

1.3 Research methodology

The methodology defined to achieve the main purpose explained formerly is described in this section.

The following tasks were conducted in the respective order to assure the success of the research:

1. Carry out a bibliographic review of adhesive bonding, giving special attention on failure prediction under different conditions and impact testing methods.

2. Design and manufacture of a heating system and a cooling system to perform the drop weight impact tests at high and low temperatures.

3. Manufacture the single lap joints for the different tests with two different bondline thicknesses to study their effect on the joints strength.

4. Perform the drop weight impact tests at the temperatures of -20, 23 (room temperature) and 80 ºC.

5. Perform tensile tests of the steel used for the adherends to determine the mechanical properties.

6. Perform bulk tests of the adhesive at different temperatures to understand the effect of the temperature on the adhesive properties.

7. Analyze and compare the results between the different conditions and obtain a suitable failure load prediction for the impact tests at different temperatures.

1.4 Thesis outline

The structure of the thesis is divided in the following sections:

Section 2: A summarized review of adhesive bonding is made, starting by describing the general characteristics of adhesives and the most typical methods to analyze the stress distributions. It is followed by a more extensive study of the effect of different factors on the joint strength, concluding with a revision of the most common impact test methods.

Section 3: The impact tests performed at different temperatures are explained here. Firstly, a description of the specimen and the test type is made. An explanation of the test procedures at different temperatures follows, including the design and manufacturing of the heating and cooling systems and the respective results.

Section 4: Tensile tests are conducted to characterize the materials used for the impact test specimens. The mechanical properties of the steel used for the adherends are displayed, while bulk tests at high and room temperature are carried to obtain the adhesive properties.

Section 5: The results are compared and discussed in this section. A failure mode prediction is made to verify the accuracy of the experimental results and try to find out a tendency in the behaviour of the specimens strength.

Section 6: A brief summary of the conclusions drawn from the other sections is made, describing the characterization obtained for the adhesive under impact load at different temperatures.

Section 7: Some ideas are mentioned to improve and continue the research of impact strength of SLJs.

2. Literature review

Even though the definition of an adhesive may vary depending on the approach chosen, it can be described, in general terms, as a material that when applied between other material surfaces is able to hold them together and resist separation [1]. There are other substances that show this phenomenon in their behaviour. Those materials which can resist significant loads are called *structural adhesives*, and their shear strength embraces a range from 5 MPa for a polyurethane to 50 MPa for an epoxy adhesive [2].

The basic structure of an adhesive joint consists in two *substrates* or *adherends*, which are the materials to be bonded, with the adhesive applied filling the gap between them. A deeper analysis of the structure describes the region between the adhesive and the adherends as the *interphase*. Inside this region there is the *interface*, a plane of contact between the surface and the two materials [1].

To study the failure of an adhesive joint, it is required to understand the difference between *adhesion* and *cohesion*. When two substances are attracted due to the intermolecular forces existing between them it is called adhesion. Cohesion will be if the intermolecular forces are established only inside one substance [1]. Thus, an adhesive joint can break by one of these or a combination of both.

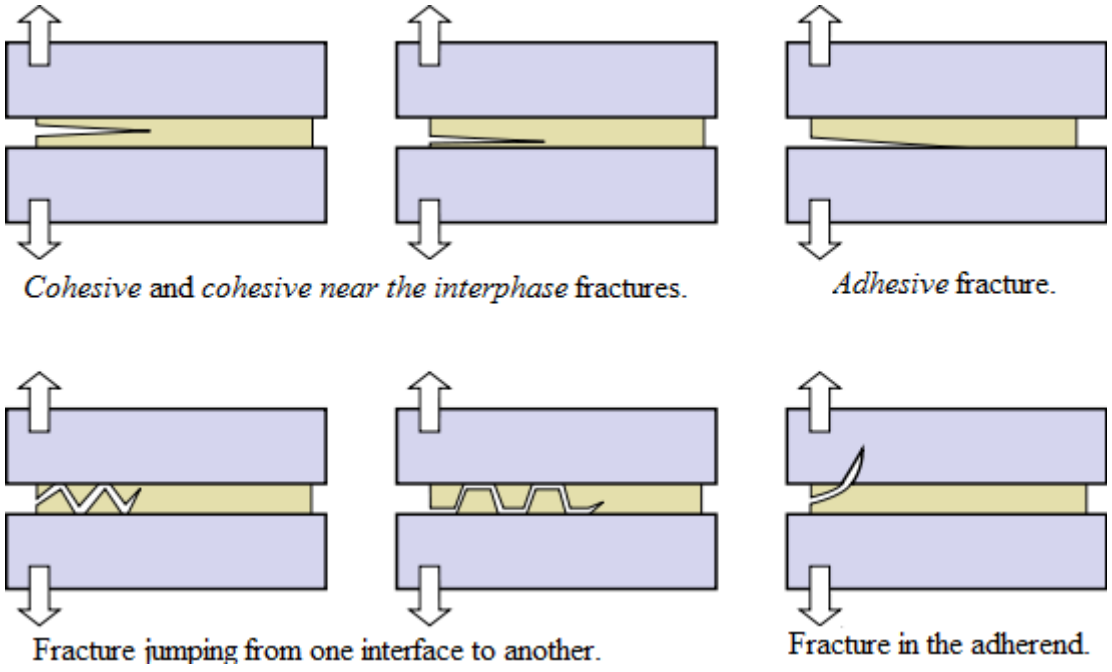

Figure 1. Examples of different types of fractures.

When a bonded joint is created, initially the adhesive is in the liquid state so that it can be easily applied on the substrates. After that, the adhesive must harden to resist the service loads, often changing its structure from a monomer to a polymer with higher molecular weight. The design of the joint and the boundary conditions will finally decide its resistance and durability [1, 3].

Once explained how an adhesive joint basically works, it is interesting to make a brief comparison with mechanical joints to understand why it is an excellent and recently increasing alternative for bonding in many cases [1].

One of the most important advantages is that the stress distribution provided by adhesive joints is more uniform over the bonded area. As a consequence, they can have the same load transmission and rigidity with less weight, reducing the cost and, referring to the automotive industry, the contamination too.

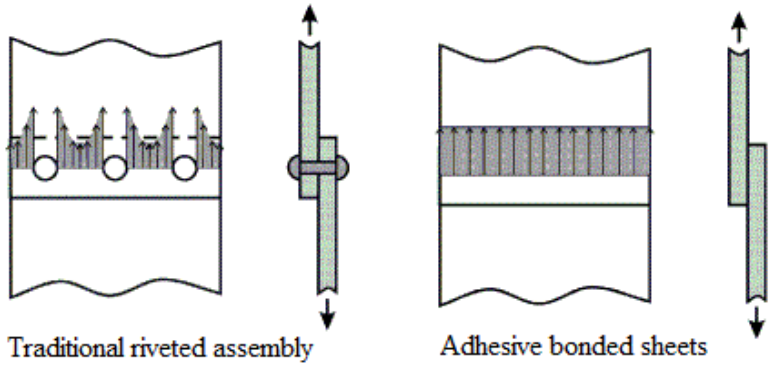

Figure 2. Stresses distribution comparison between mechanical and adhesive joint [1, 3].

In addition, adhesives can bond materials with different coefficients of thermal expansion because of their flexibility, and they are able to join very thin plates too, allowing them to be used to build very light but resistant structures, which makes them very suitable for a great sort of applications such as transportation. Concerning to their implementation in fabrication processes, they are highly efficient because it is easy to create an automatic process to apply them [1].

However, the use of adhesive bonding in some areas entails also some disadvantages that need to be improved or eliminated, which is another reason to continue researching this technology. To begin with, adhesive joints are more sensitive to temperature and humidity than mechanical fasteners, showing limited resistance in extreme conditions.

Their design needs to avoid some particular load cases, as cleavage and peel stress, and localized stresses [3]. Figure 3 shows the different type of stresses that can appear in an adhesive joint with the typical configurations used to design them.

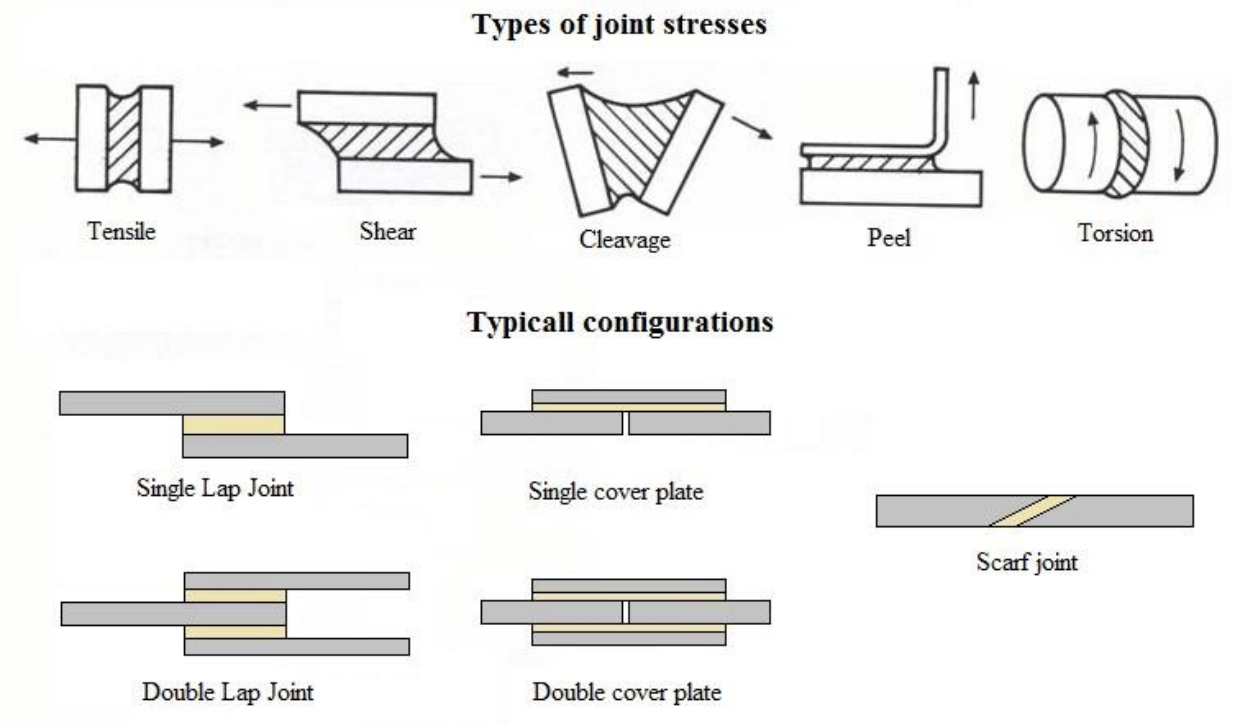

Figure 3. Types of stresses and typical configurations [1-5].

2.1 Adhesive joint properties

To understand why the selection of the adhesive is a key step in the design of an adhesive joint, it is essential to know how many possibilities are available. In order to make this choice easier, adhesives have been classified in categories depending on the approach [1].

A first classification divides them by their origin, so that they can be *natural* or *synthetic*. Natural adhesives are produced or extracted from the natural resources, as starch, casein glues or natural rubber. Synthetic adhesives are those designed and made by the industry and all of them are based on polymers.

The functionality on the polymer once it has been cured classifies the adhesives in *thermoplastics*, *thermosets* and *elastomers* (rubbers). This depends on the strength of their intermolecular bonds and molecular structure. One of the main differences in their behaviour lies on their glass transition temperature (T_g).

Regarding to the final role of the adhesive there are two important groups to distinguish; the *structural* and the *non-structural*. Structural adhesives are mostly one- or two-component thermosetting resins and are meant to resist stresses significantly higher than the ones under service environment. On the other hand, non-structural are divided in other groups depending on their application, as hot melt, pressure sensitive or water-base adhesives [1].

Finally, other adhesive classifications exist based on the different chemical families (epoxy, silicon), their physical form (one or multiple components) or their type of curing method [1, 4].

2.1.1 Structural adhesives

Due to the purpose of this study a brief review focusing in structural adhesives has been done. Generally, structural adhesives are cross-linked/thermosetting polymers even though some can be thermoplastic. To be considered structural, the adhesive shear strength must vary from 5 to 50 MPa [2].

Properly made adhesive joints are supposed to fail by the adhesive, likely by cohesion. Moreover, in most cases the adherends are made of stiffer materials than the adhesive and, as a consequence, almost all the elongation is due to the strain in the adhesive. For this reason, the strength of most of the adhesive joints is related to the strength of the adhesive.

It is relevant to understand the difference between adhesive strength and joint strength. Adhesives which are more ductile and flexible are generally weaker than stiffer ones but, when they are applied in the joint, they use their ductility to redistribute the stress along the overlap, causing a plastic deformation in the joint. Therefore, joints with ductile adhesives can be much stronger than others with stronger but less ductile adhesives [1, 5].

Considering this, it is important to know the characteristics of the different structural adhesives in order to select the optimum for each application. A summary of the most common structural adhesives mechanical properties is shown in Table 1, followed by some other interesting features [1-6].

Table 1. Typical values of some mechanical properties of structural adhesives [1-6].

Mechanical properties of common structural adhesives

Adhesive type	Young's modulus (GPa)	Shear modulus (GPa)	Tensile strength (MPa)	Density (kg/m^3)	Elongation (%)
Epoxy	2.5	1.2	60	$1.15 \cdot 10^3$	4
Polyurthane	0.02	0.008	40	$1.18 \cdot 10^3$	650
Phenolic	3.5	1.4	50	$1.4 \cdot 10^3$	1
Silicone	0.001-0.005	0.004	10	$0.98 \cdot 10^3$	700

- **Epoxy (EP):**

Service temperature: -40ºC to 100ºC for one-part, -40ºC to 180ºC for two-part epoxies.

Physical forms: One-part system, Two-part system.

Advantages: high strength, excellent toughness, corrosion resistance and dimension stability, good dielectrical properties and low shrinkage.

Disadvantages: occasional voids and slow curing for two-part epoxies, storage and need to cure at high temperature for one-part epoxies.

Applications: aircraft, helicopters, trains, vehicles, sports training, etc.

- **Polyurethanes:**

Service temperature: -40ºC to 80ºC

Physical forms: One-part system, Two-part system.

Advantages: excellent resistance to abrasion and tear, wetting ability and excellent strength and toughness at low temperatures.

Disadvantages: poor resistance to heat and moisture cure.

Applications: automotive industry, cryogenic applications, shoe industry.

- **Phenolics:**

Service temperature: -40ºC to 160ºC

Physical forms: Nitrile-, polyvinyl-, neoprene-phenolics.

Advantages: high hardness, excellent thermal stability and dielectric properties.

Disadvantages: brittle, porous bondline and difficult processing.

Applications: automotive parts, wiring devices, wood industry, etc.

- **Silicones:**

Service temperature: -70ºC to 250ºC

Advantages: temperature range, electrical properties, environmental stability.

Disadvantages: poor strength, poor resistance to abrasion, fuel, oil and hydrocarbons and high cost.

Applications: food process equipment, glass assembly and electrical insulation.

Although these are indicative values and the variety of adhesives in each group is very wide, it is helpful to have an idea in the beginning of the selection of the adhesive. However, there are other important factors to take into account when it comes to choose a specific adhesive, as the substrates material, surface pre-treatments needed, costs, application process, etc. This implies how much experience is required when choosing the optimum adhesive for each application.

2.1.2 Adherend properties

Focusing on the adherend material, it has been said before that properly made adhesive joints tend to fail by the adhesive because its strength is usually lower than the material of the adherend. However, for some applications, it is required to bond more flexible materials because some elongation is needed in them in order to absorb more energy when they are stressed.

Furthermore, when loaded over a large area such a single lap joint, the adhesive can provide a high joint strength, enough to make the metal deform instead of the adhesive [1, 3, 6]. As a consequence, the substrates material in some adhesive joints can behave in a more ductile and weaker way under load than the adhesive. Thus, the strength of these adhesive joints is related to the strength of the adherents or a combination of both.

An overview of the most common materials used for the substrates has been done, showing the typical values for their mechanical properties in Table 2. The most important are the adherend modulus and its strength. Adherends with low modulus suffer high deformations at the end of the overlap, where the load transfer appears, causing a higher effect due to the differential straining in the adhesive [1, 3]. The strength is essential and gives information about the joint failure, since it is known that the adherend yielding can lead to failure.

Table 2. Common substrates materials properties from ASTM steel and composite standards.

Material	Young's modulus (GPa)	Shear modulus (GPa)	Tensile strength (MPa)	Elongation at break (%)	Relative density
Mild steel	205	80	370	15	7.9
Hard steel	200	80	650	25	7.8
Aluminium	70	25	275	12	2.7
Carbon fiber composite (Std. CF)	70	5	600	0.85	1.6

2.1.3 Thermal properties of adhesives

Temperature has an important role in adhesive bonding due to the sensitivity of most of adhesives to it, whether regarding to the curing process or when they are in service. The critical value when referring to temperature is the glass transition temperature, reason why it is of vital importance to know it and to avoid crossing it when the joint is being used [1].

Adhesives when applied are in the liquid state so that it is possible to properly wet the adherends. To solidify the adhesive into a cohesive mass it must pass through the *hardening* or *curing* process. Curing can be done in different ways, depending on the type of the adhesive. Hardening by evaporation of solvent or water is one of them, which consists on using the low heat of evaporation of the solvents to eliminate the liquid in the adhesive. Latex adhesives also cure by loosing liquid, since their structure consists in very little particles suspended in an easily absorbable substance. Another type of curing is the hardening by cooling, where the hot-melt adhesives are first heated to reach liquid state and be applied and then they are cooled. Finally there is the curing by chemical reaction, which depends on the temperature applied to the adhesive, and it is used for epoxies, structural acrylics, cyanoacrylates, silicones and high temperature adhesives [1, 3].

Once the adhesives have been cured they are ready to be used, which is why it is essential to describe their thermal properties at this point. As explained before, the most important parameter to consider for all polymers is the *Tg*. At low temperature most of the adhesives remain in a glassy state, behaving brittle and inflexible. Above the glass transition, this state changes into a rubbery or leathery one and the adhesive becomes soft and flexible and, consequently, structurally useless, nevertheless there are some adhesives, as rubbery-based ones, which are used in the leathery state [1].

Although each adhesive has its own *Tg*, all of them have very sensitive properties to temperature variation. Figure 4 shows how the tensile shear strength of some typical adhesives varies with temperature.

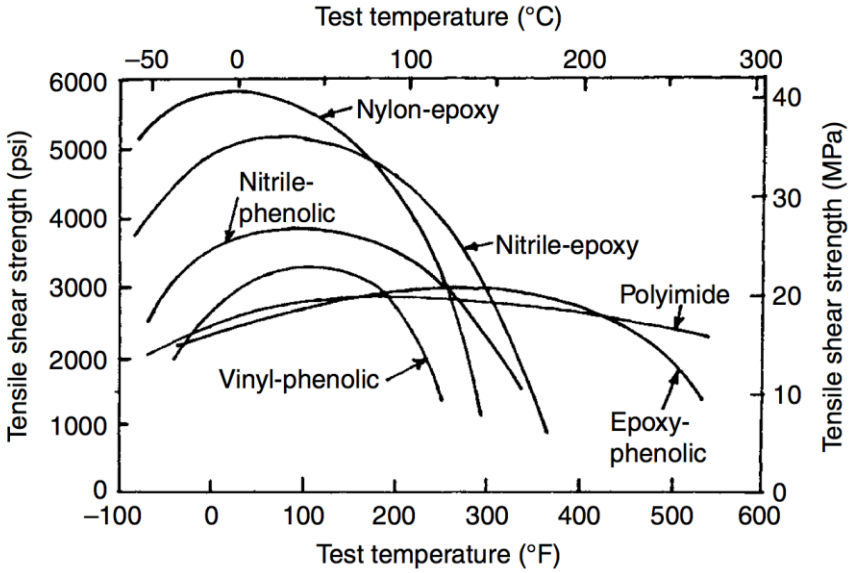

Figure 4. Effect of temperature in the tensile shear stress of different adhesives [5].

The crystalline melting temperature is not considered as important as glass transition. This is because most of adhesives are made of polymers with amorphous structure as a consequence of a lack of molecular regularity [1].

Another important property of adhesives is their thermal expansion coefficient, which tend to be much greater than those of the materials of the adherends. Thus, when joints with large overlaps remain at high temperature during time the difference between the areas bonded becomes relevant, harming the bond stresses. When bonding dissimilar materials the thermal stresses are especially relevant, due to the different thermal expansion coefficients [1, 3].

2.2 Analysis of Single Lap Joints

Understanding the mechanics of failure in adhesive bonding is essential to improve design and obtain much stronger joints. The objective when studying different analytical approaches is to achieve the most accurate failure prediction by determining the joint stress distribution and its strength.

There are two ways to predict the stress distribution in an adhesive joint. The first one and more accurate is by a numerical method as the finite element analysis (FEA). When the adhesive joint has a complex geometry or the materials are elaborate this is the most suitable choice. For a faster and easier prediction, the second solution is to use a closed-form model [1, 7].

Due to the main purpose of this study, only a review of the simplest analytical models for single lap joints (SLJ) is done. Moreover, single lap joints are the simplest geometric configuration and they have been used as a standard testing specimen to characterize the adhesive properties. In spite of this, it is interesting to know the existence of more analysis for other kind of joints, such as the models from Adams and Peppiatt, Lubkin and Reissner and Nems et al. for tubular joints [7, 8].

When using SLJs, failure usually appears in the adhesive. Thus, a lot of literature of different researchers can be found concerning the stress distribution in this region. Depending on the approach, a SLJ can be described in a two-dimensional (2D) analysis or in a three-dimensional (3D). In the latter numerical methods are needed while in the former some simplifications can be done, as restricting the adhesive stresses to peel and shear and consider only tension and bending to explain substrates deformation [1].

2.2.1 Basic linear elastic analyses

This simplest analysis of a SLJ describes the adherends as rigid bars compared to the adhesive, which is treated as a substance much softer. Figure 5 shows that the deformation only appears in the adhesive in shear, and the shear stress is considered constant along the overlap, which can be interpreted as an average value on the adhesive layer [7].

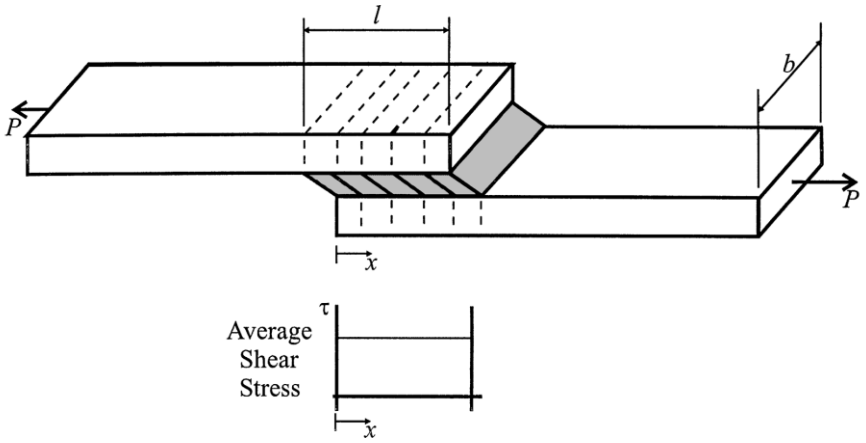

Figure 5. Adhesive deformation in SLJs with rigid adherends and constant shear stress [9].

The value of the shear stress is calculated by:

$$\tau = P/bl \quad (1)$$

Where P is the applied tensile force, b is the joint width and l the overlap length. Although this is not a very accurate analysis because of its simplifications, it is still used to quote the adhesive shear strength in quite a few tests situations [1, 7].

2.2.2 Volkersen's analysis

The shear lag model proposed by Volkersen [10] also considers the adhesive deformation in shear, but adds the deformation in tension in the substrates. This is because in this case the adherends are considered elastic instead of rigid. This differential shear in the adherends is shown in Figure 6, where the maximum tensile stress appears at A, decreasing progressively to B.

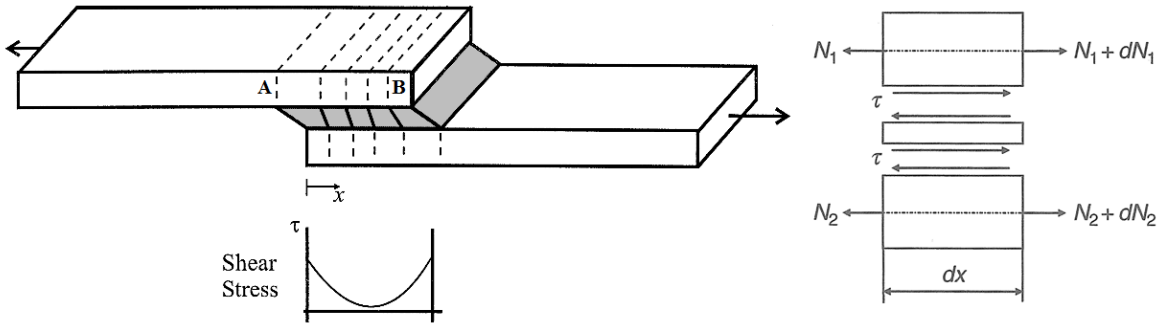

Figure 6. SLJs with elastic adherends deformations (left) and free body diagrams (right) [1, 9].

Due to this reduction of the strain along the overlap, a non-uniform shear strain and stress distribution in the adhesive layer is produced. The equation that gives the shear stress is:

$$\tau = \frac{P\ w\ cosh(wX)}{bl\ 2\ \sinh\ (w/2)} + \left(\frac{\psi - 1}{\psi + 1}\right)\frac{w\ sinh(wX)}{2\ \cosh\ (w/2)} \quad (2)$$

Where

$w^2 = (1 + \psi)\phi$

$\psi = t_t/t_b$

$\phi = \frac{G_a l^2}{E t_t t_a}$

$X = x/l\ , \quad -\frac{1}{2} \leq X \leq \frac{1}{2}$

Where t_t is the top adherend thickness, t_b the bottom adherend thickness, t_a the adhesive thickness, *E* the adherend modulus and G_a the adhesive shear modulus [8].

The shear stress distribution along the overlap as a result of these equations is shown in Figure 6, where the maximum stress is located at the ends of the overlap. However, for single lap joints this model doesn't consider the moment that appears because of the non-colinearity of the applied loads. Thus, this method is more suitable for double lap joints, since their bending moment is not as significant as the one that SLJs suffer [1, 7, 8].

2.2.3 Goland and Reissner's analysis

The adhesive-beam model proposed by Goland and Reissner [11] features the adhesive as a two-parameter elastic medium, and the adherends as Euler beams. In this case it is considered that the bending moment (*M*) and the transverse force (*V*) applied at the joint ends are caused by the eccentric load path of a SLJ. Figure 7 presents the model in a SLJ showing the deformations over the overlap due to this characterization and the stress analysis [7].

This bending moment makes the joint rotate and, as a consequence, the load applied is no longer aligned with the shear planes in the bond. Furthermore, the bending moment decreases as the joint rotates and the effects of large deflections of the adherends are taken into account [7].

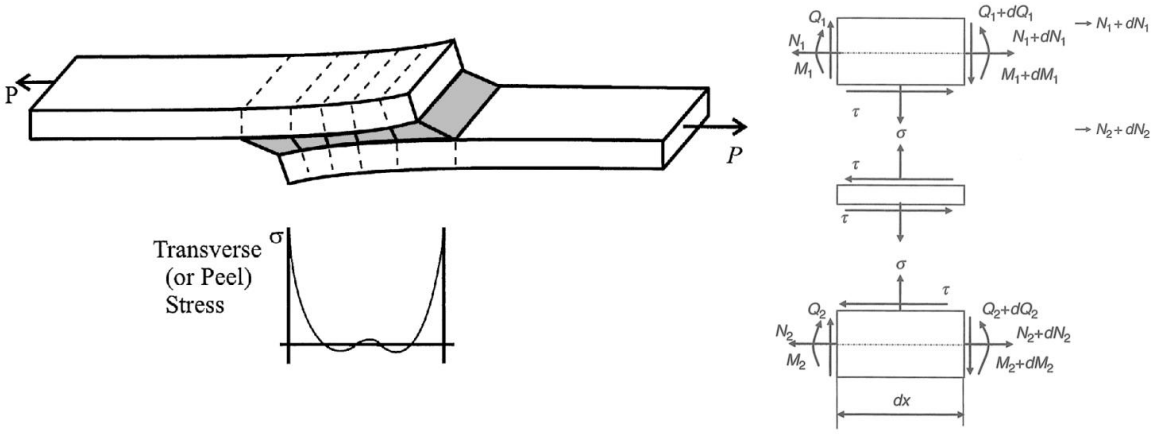

Figure 7. SLJs stress distribution (left) and free body diagrams (right) with Goland and Reissner's model [1, 9].

The bending moment factor (k) and the transverse force factor (k') are used to consider this phenomenon, so that they give a relation between the tensile load applied per unit width ($\bar{P}$) and the bending moment and the transverse force at the overlap ends. Accordingly, if the joint does not rotate the value of these factors is 1 and as it rotates it decreases to 0. The bending moment and the transverse are given by

$$M = k\frac{Pt}{2} \quad (3)$$

$$V = k'\frac{Pt}{2c} \quad (4)$$

The adhesive shear stress is obtained by the following equation

$$\tau = -\frac{1}{8}\frac{\bar{P}}{c}\left\{\frac{\beta c}{t}(1+3k)\frac{\cosh\left(\left(\frac{\beta c}{t}\right)\left(\frac{x}{c}\right)\right)}{\sinh\left(\frac{\beta c}{t}\right)} + 3(1-k)\right\} \quad (5)$$

where c is half of the overlap length ($l/2$), t the adherend thickness,

$$\beta^2 = 8\frac{G_a}{E}\frac{t}{t_a}$$

$$k = \frac{\cosh(u_2 c)}{\cosh(u_2 c) + 2\sqrt{2} sinh(u_2 c)}$$

$$u_2 = \sqrt{\frac{3(1-v^2}{t}} \frac{1}{t} \sqrt{\frac{\bar{P}}{tE}}$$

And the adhesive peel strength is given by:

$$\sigma = \frac{\bar{P}t}{\Delta c^2}\left[\left(R_2\lambda^2\frac{k}{2} + \lambda k'\cosh(\lambda)\cos(\lambda)\right)\cosh\left(\frac{\lambda x}{c}\right)\cos\left(\frac{\lambda x}{c}\right) + \left(R_1\lambda^2\frac{k}{2} + \lambda k'\sinh(\lambda)\sin(\lambda)\right)\sinh\left(\frac{\lambda x}{c}\right)\sin\left(\frac{\lambda x}{c}\right)\right] \quad (6)$$

where *x* is the origin of the longitudinal co-ordinate in the middle of the overlap and

$$\lambda = \gamma\frac{c}{t}$$

$$\gamma^4 = 6\frac{E_a}{E}\frac{t}{t_a}$$

$$k' = \frac{kc}{t}\sqrt{3(1-v^2)\frac{\bar{P}}{tE}}$$

$$R_1 = \cosh(\lambda)\sin(\lambda) + \sinh(\lambda)\cos(\lambda)$$

$$R_1 = \sinh(\lambda)\cos(\lambda) - \cosh(\lambda)\sin(\lambda)$$

$$\Delta = \frac{1}{2}(\sin(2\lambda) + \sinh(2\lambda))$$

This solution introduces the importance of the bending moment in case of SLJ analysis and the necessity to bear in mind the peel stresses despite the simplifications of shear and normal deformations in the adherends. Then it is deduced that the Goland and Reissner's [11] analysis is for adhesively bonded isotropic joints.

Hart-Smith [12] though developed this model by considering deformations in the adherends too, giving a new expression for the bending moment factor (*k*) value:

$$k = \left(1 + \frac{t_a}{t}\right)\frac{1}{1 + \xi c + \frac{1}{6}(\xi c)^2}$$

where *D* is the adherend bending stiffness and $\xi^2 = (\overline{P}/D)$.

Another expression for the bending moment factor much simpler was developed by Zhao et al. [13] more accurate for thick and stiff adherends but not suitable for short overlaps as:

$$k = \frac{1}{1 + \xi c}$$

As a conclusion, when comparing the models of Volkersen [10] and Goland and Reissner [11] it is observed that, even though both give similar shear stress distributions, the latter solution predicts higher adhesive shear stress at the ends of the overlap [7, 8]. Furthermore, although they were a big progress in the analysis of the stress in adhesive joints, they still have some limitations that have been studied and improved by several researchers.

2.3 Failure prediction

It is known that the stress distribution is not uniform along the adhesive overlap. Then that local stresses can be higher than the average shear stress of the adhesive, provoking an unexpected failure in the joint. Some general guidelines can be followed to improve the strength in adhesive joints, as using and adhesive with low modulus and ductile behaviour, using a thin adhesive layer or a large bonded area. However, for most structural applications it is essential to predict accurately the moment of the failure in the joint [1].

When designing strong SLJs for the automotive industry, there are some factors that are significant, as the material selection for the adherends and the adhesive and how parameters such as the thickness, the overlap length or the temperature affect them.

In this section a brief review of the effect of these parameters in SLJ failure has been done, in order to allow a more accurate understanding of the results of the experimental work.

2.3.1 Adhesive and adherend properties

Regarding to the adhesive properties, it has been mentioned before that although ductile and flexible adhesives are generally weaker than stronger but less ductile adhesives, they become more suitable when used in adhesive bonding. Their ductility and flexibility allow them to give a more uniform distribution of the stress along the overlap than stiffer adhesives (see Figure 8), which leads to stronger joints [1, 14].

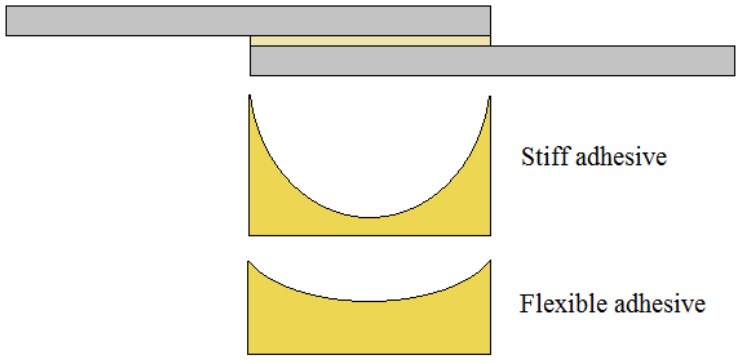

Figure 8. Adhesive stress distribution as a function of the adhesive modulus [1].

Generally it is better to use ductile adhesives because their durability under fatigue is higher than that of brittle ones [1]. However, other factors such as the overlap length can change these considerations, as it will be shown later.

When it comes to adherends, the parameters with the greatest impact on the adhesive joint strength are the modulus and their strength. It is deduced from Volkersen's analysis that the deformation at the ends of the overlap determines the variation of the strain in the adhesive. Thus, a high adherend modulus will reduce these deformations and provide less differential straining in the adhesive [7].

The adherend strength has an important role in the joint failure. As described later in Adams et al. [14] failure prediction, adherend yielding makes the joint break sooner than with global yielding of the adhesive along the overlap. If the stress in the adherend reaches the yield point of the metal at the ends of the overlap (Figure 9), it begins to plastically deform, until the maximum strain in the adhesive is reached and the joint fails [15].

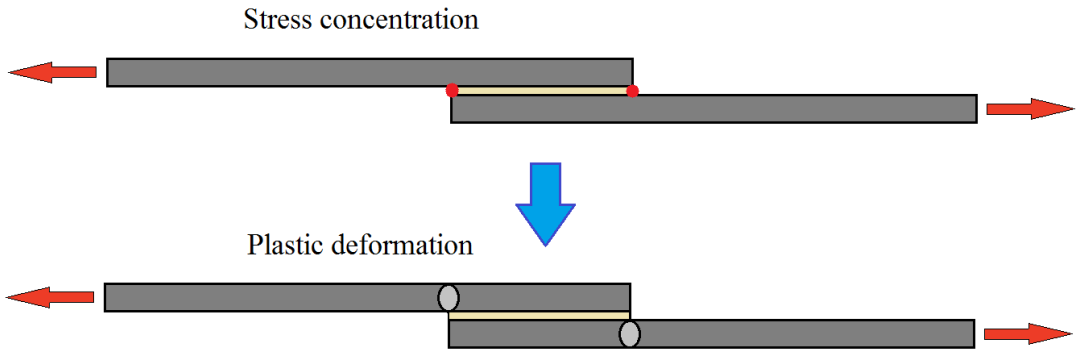

Figure 9. Adherend yielding in a single lap joint [1].

Then, for SLJs with ductile steel substrates the failure load predicted will be lower than that with hard steel adherends. As an example of this, Figure 10 shows experimental results of load failure comparing different adherend materials [15].

However, in the automotive industry, ductile steel is generally used in cars structure because of the need of deformation in case of accident, so that the energy absorbed by the car is much higher than the passengers inside. Therefore, it is important to analyze adherend yielding in SLJs.

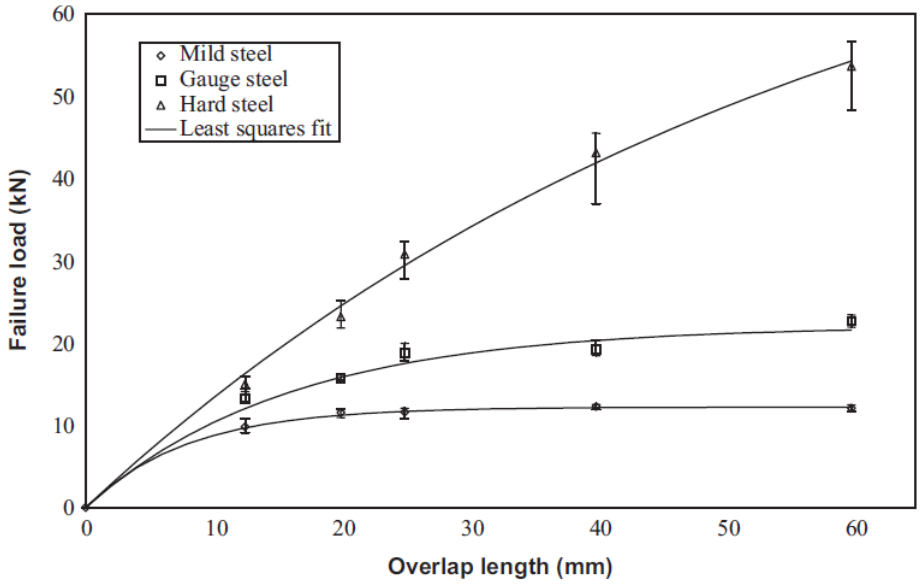

Figure 10. Strength of SLJs in tension vs. overlap length for different adherend materials and an adhesive of moderate ductility (10% in tension) [15].

2.3.2 Adhesive thickness

According to the analytical models of Volkersen [10] and Goland and Reissner [11], the bondline thickness should improve the joints strength when increased. Experimental results documented in the literature show the opposite though. For structural adhesives under tension, the optimum thickness seems to be in the range of 0.1-0.2 mm and with higher values the failure load decreases [1], as seen in Figure 11.

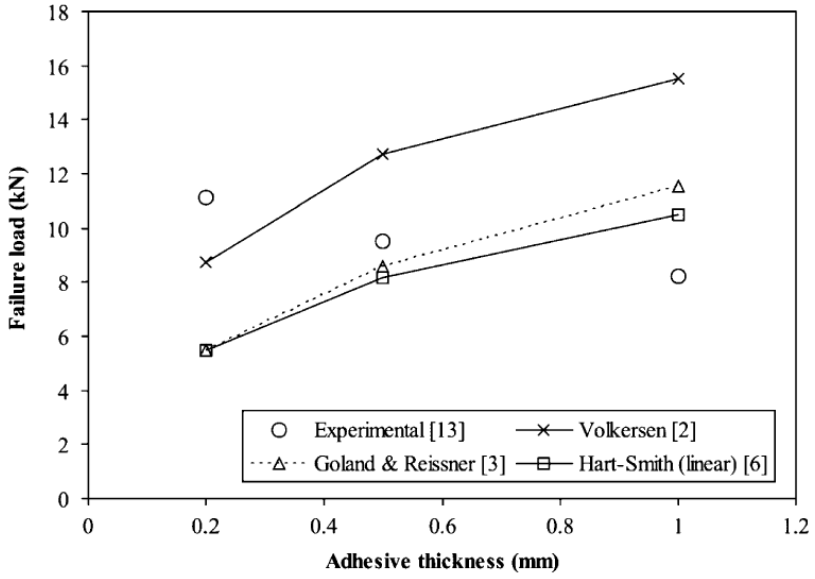

Figure 11. Experimental results vs. analytical models in function of adhesive thickness [8].

The reasons for this contrast between the analytical models and the real results have been studied by several researchers. Despite many theories, the one that explains it better was developed by Grant et al. [16]. In the FEA results shown in Figure 12 it was demonstrated that the strength decreases when the bending moment increases.

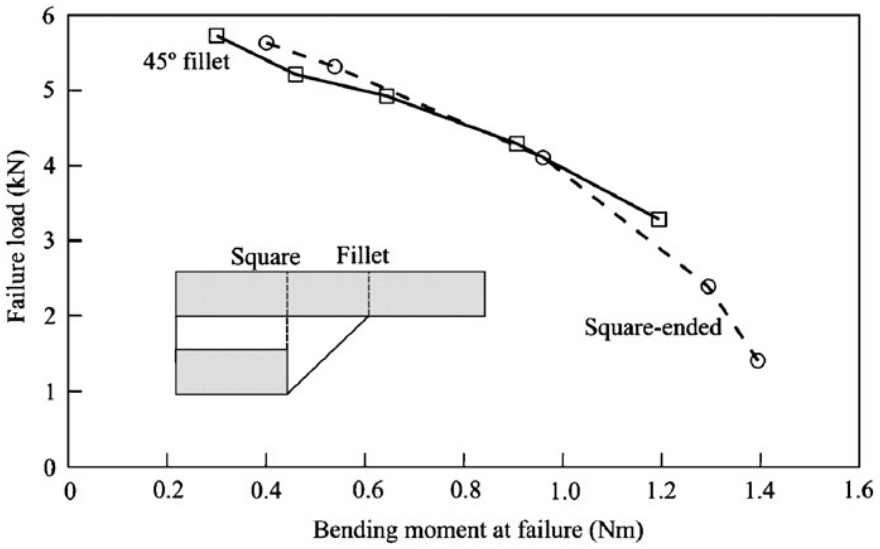

Figure 12. Failure load vs. bending moment for lap joints under tension (FEA results) [16].

Since the thicker the bondline, the higher bending moment appears when loaded in tension, the lower is the strength in the joint (see Figure 13) [17].

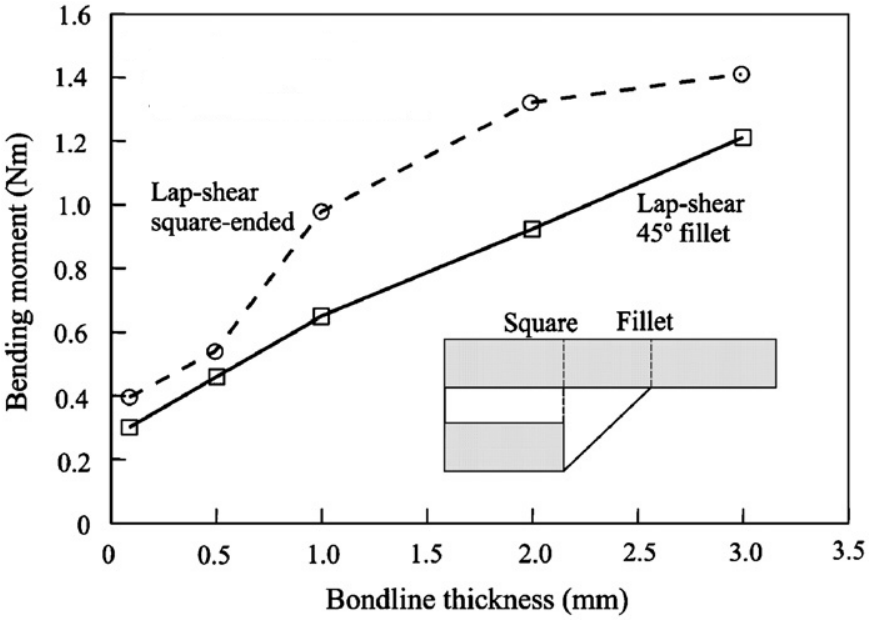

Figure 13 Bending moment vs. bondline thickness [16].

2.3.3 Overlap length influence

To study how the length of the adhesive overlap affects the failure the dependence on the adhesive and adherends materials must be taken into account, which establishes three cases to consider:

- *Elastic adherends with ductile adhesive*. The joint strength is almost proportional to the overlap length. The adhesive deforms plastically and as the load increases it redistributes the stress. This case of failure is considered global yielding in the adhesive.

- *Elastic adherends with brittle adhesive*. The joint strength is not proportional to the overlap length. The stress concentrates at the ends of the overlap and increasing the overlap length does not vary the stress distribution.

- *Adherends that yield*. The adherend yield strength determines the failure so that the bending moment, which depends on the overlap length, acquires an important role.

Adams et al. [14] developed a failure predictive model addressed to SLJs under tension. For overlaps lengths up to 40 mm and bondlines thinner than 1 mm it has been experimentally demonstrated that it fits well enough with the experimental results. For longer overlaps, more complex analytical methods are needed. However, of the three cases mentioned before, this model only considers the adhesive global yielding and the adherend yielding. For brittle adhesive the Volkersen's model is more suitable [7].

When using elastic adherends and ductile adhesives, the failure load predicted is attributed to the total plastic deformation in the adhesive (global yielding), and it is given by

$$P_a = \tau_y b l \quad (7)$$

where P_a is the failure load of the joint , τ_y is the adhesive yield strength, b is the joint width and l the overlap length. The shear yield stress of the adhesive can be deduced from the tensile yield stress assuming a von Mises yield model as a first approximation. The direct tensile stress σ_t acting in the adherend due to the applied load P is

$$\sigma_t = P/bt \quad (8)$$

where t is the adherend thickness. If a bending moment (M) appears, the stress at the inner adherend surface follows the equation

$$\sigma_s = 6M/bt^2 \quad (9)$$

where according to Goland and Reissner's model $M = kPt/2$. The bending moment factor (k) is reduced from unity as the lap rotates under load. The global stress acting in the adherend is calculated as the sum of this two stresses and, as a result, the maximum load failure for adherend yielding is

$$P_y = \sigma_y bt/(1 + 3k) \quad (10)$$

where σ_y is the yield strength of the adherend. For low loads and short overlaps the value of the bending moment factor is 1. If the relation between the overlap and the bondline thickness is $l/t \geq 20$ its value is considered 0 [8].

Figure 14 represents graphically these equations and the linear relation between overlap length and failure load in adhesive joints with non-yielding adherends and ductile adhesives can be seen. For yielding adherends, the k factor can be estimated for overlaps which are not very short or very long, so that a more accurate prediction can be obtained [1, 8, 17].

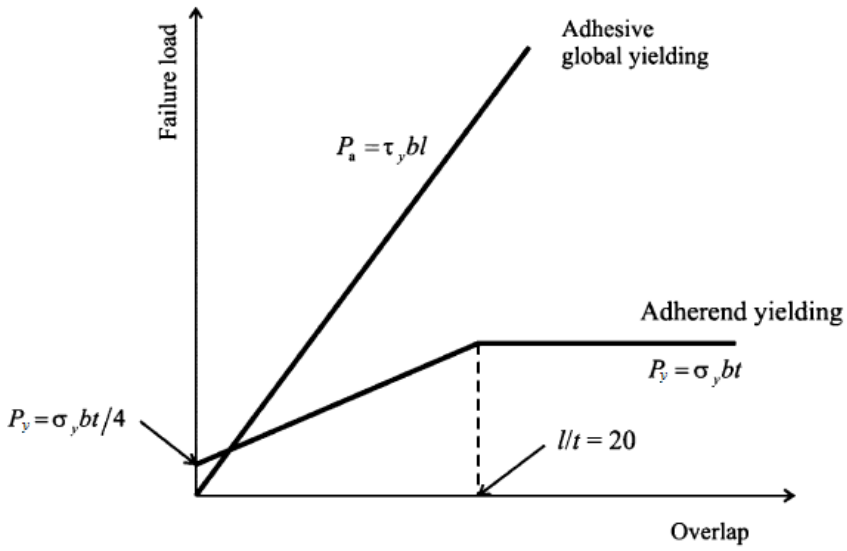

Figure 14. Failure load vs. overlap length by Adams et al. failure prediction model [8].

2.3.4 Effect of temperature

In the automotive industry, one of the most important factors in adhesive bonding that must be considered is the temperature variation. It is essential to be able to predict how the mechanical properties of adhesives vary with temperature and strain rate due to their polymeric nature. It has been demonstrated that the joint strength depends on temperature, especially near the glass transition temperature (*Tg*) of the adhesive [1].

The coefficients of thermal expansion (CTE), especially when compared to the CTE of dissimilar substrates, and adhesive mechanical properties with temperature are the most significant characteristics that decide the adhesive joint strength when used under a wide temperature range [18, 19, 20, 21].

The properties of adhesives and sealants over the range of service temperatures need to be studied for each type of application. For example, the adhesive joints used in automotive industry need to withstand temperatures between −40 and 90ºC, so the adhesives stress–strain data must be characterized over the range of these temperatures [16].

Experimental results in different studies with structural adhesives (especially epoxies) show that under higher and lower temperatures their joint strength is decreased. When an adhesive joint with dissimilar adherend materials is working at high temperature, the cause of its weakness is the low adhesive strength, while when the temperature is decreased it is due to the high thermal stresses. On the contrary, when SLJs with similar adherend materials are submitted to low temperatures, adhesive brittleness becomes relevant. For SLJs

with an epoxy adhesive tested at low temperature, results show that the joint stiffness is more affected by the response of the adherends than by the modulus of the thin adhesive layer [22].

Some recent studies testing SLJs with adherend yielding and a ductile adhesive at low and high temperature have been done. The results represented in Figure 15 show that the strength at room temperature is higher than at high temperature, but lower than at low temperature. The explanation is that at high temperature the joints are weaker because the yield point of the adherend is at a lower stress than at room temperature, while at low temperature the adherend yields at higher stress, making the joint stronger [16].

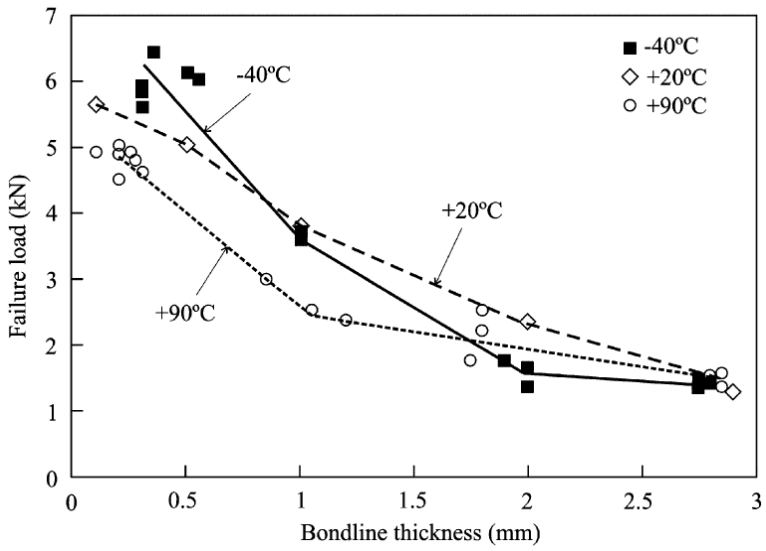

Figure 15. Single lap joints tested in tension at +90, +20 and -40 ºC [16].

2.3.5 Impact load

Studies of impact phenomenon on SLJs are increasing recently in the automotive industry. It is crucial under impact load to transfer the load without fracturing the joint thus assuring the integrity of the car under a crash situation. Moreover, more attention must be given to the energy absorbed by the joint when an impact load is applied, since the priority in a crash situation is that the car structure absorbs the maximum energy as possible to keep the passengers safety [23].

When SLJs are submitted to high strain-rate conditions, their material properties tend to be different from the ones reviewed in quasi-static conditions [1]. Thus, it is hard to accurately predict failure for impact loads. However, experimental results for impact

tests can be found in the literature and, if the characteristics of the adherends and adhesive materials are similar to those obtained in static conditions, it is possible to extrapolate them to predict failure.

Results were found for drop impact load tests in SLJs with a high elongation epoxy adhesive and ductile adherends. Under high strain-rate the failure mode obtained was almost the same as that in quasi-static tests, although some differences in the behaviour were noticed. The adherends deformed less than in quasi-static tests, absorbing less energy, due to their sensitivity to the high strain-rate. As a result the failure load increased but the adhesive experienced similar damage as in the quasi-static tests (see Figure 16) [23].

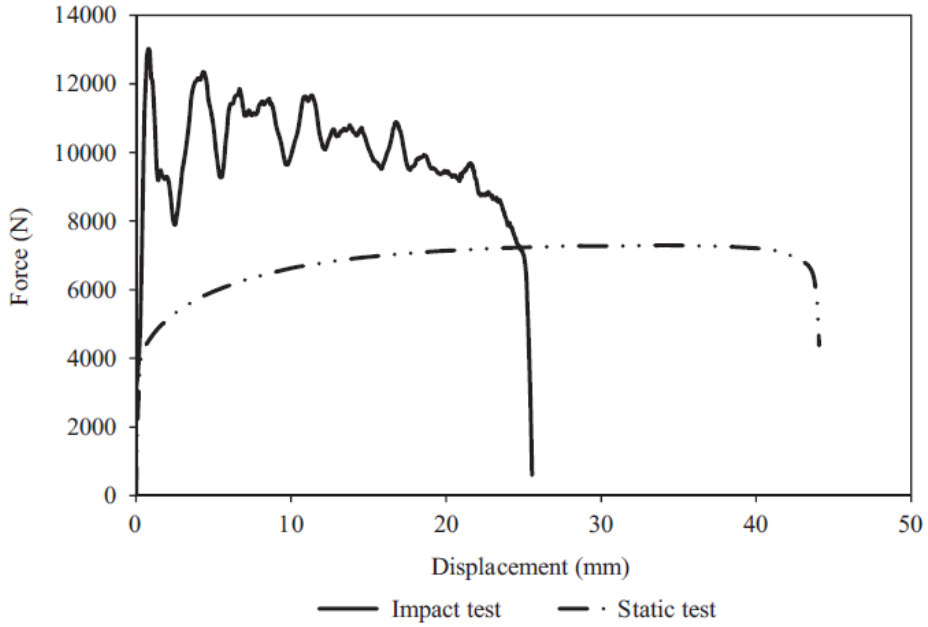

Figure 16. Comparison of SLJ with mild steel adherends under different strain rates (1 mm/min for static and 4.47 m/s for impact) [23].

Harris and Adams [24] obtained impact results for lap shear aluminium alloy specimens, observing that the adhesive held together the adherends while they deformed plastically in tension. Results of energy absorbed and failure load for different combinations of adhesive and adherend materials are shown in Figure 17.

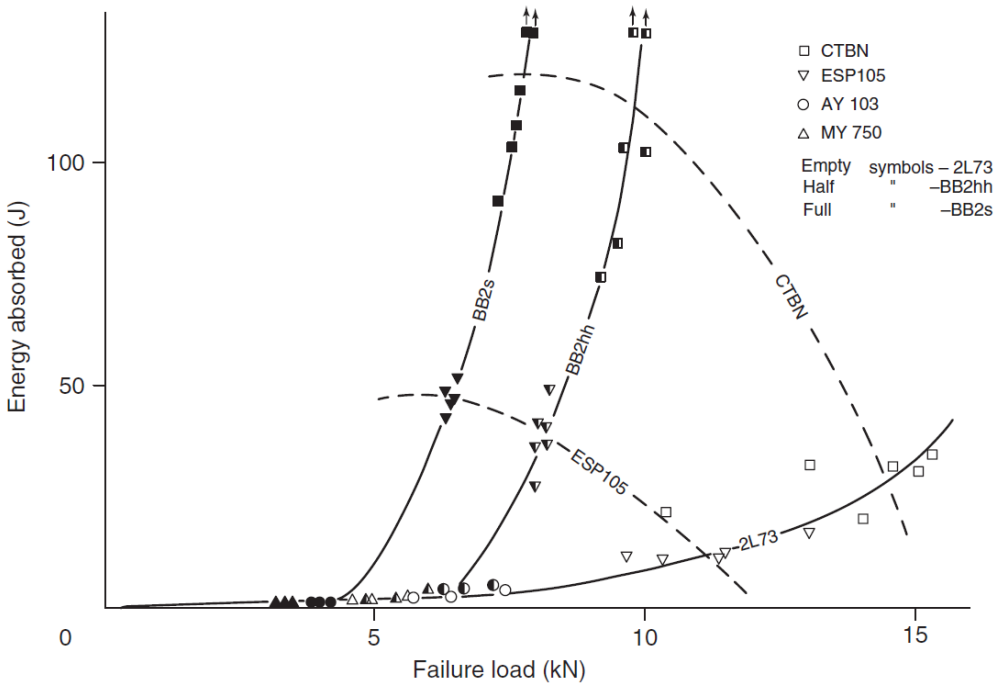

Figure 17. Instrumented pendulum impact results for lap shear aluminum alloy specimens [24]**.**

It was noticed that using rubber-toughened adhesive with ductile aluminium alloy adherends provided the highest energy absorption, while for a high-strength aluminium alloy, the joint strength increased with a reduction of the energy absorption due to the high yield strength of the aluminium [24]. Thus, when the adhesive used is strong enough to keep the adherends together under impact load, it is also the adherend yielding that controls failure.

In conclusion, at room temperature, when using ductile with strong and ductile adhesives, the sensitivity of the adherend material to the high strain-rate is what determines failure. When temperature varies enough to decrease the adhesive strength while impact loading, failure is controlled by the adhesive sensitivity to high strain-rate. In this case, knowing the adhesive properties as a function of temperature is essential to accurately predict failure.

For a ductile epoxy adhesive working at low temperature a more brittle behaviour is expected with a decrease of its mechanical properties too. Thus, the model that should be used to predict failure is Volkersen [10]. On the other hand, when this adhesive is impact loaded under high temperature, it is expected to be more ductile and less strong. In this case, model Adams et al. [14] for adhesive global yielding could be used.

2.4 Test methods

To properly create, select and predict the performance of adhesives for different applications a characterization of the adhesive physical properties is indispensable. Although the analytical models are becoming more accurate over recent years, testing the adhesive is always essential, as it provides real results that in some cases are unexpected or unpredictable. Tests can be performed to check the properties of an adhesive as a quality control, to put the adhesive under extreme conditions or as a part of the process of design [1].

The quantity of methods available to determinate the failure strength data is wide. In general terms though, they are divided in two groups: test on bulk specimens and tests in a joint or *in situ*. In the former the specimen to test is a piece of cured adhesive and the performance follows the standards for plastic materials. In the latter the adhesive is tested once it has been cured in the joint, so that it represents the adhesive joint under different conditions more in accord to reality [25]. In this study, a brief review of different test methods has been conducted, paying more attention on impact tests due to the main purpose of the thesis.

2.4.1 Quasi-static testing of bulk specimens

The tensile test on bulk specimens is usually carried out to determine the strength properties of an adhesive. It consists on applying a uniform and uniaxial stress in the adhesive without the influence of the adherends, obtaining results of its properties that, even though they may vary from the *in situ* tests, are useful for the adhesive selection and to predict failure [25].

I. Specimen geometry

There are different geometries for the bulk specimen to test according to the standards depending on the material of the adhesive. The usual geometry is the dogbone-shaped

specimen that follows the EN ISO 527-2 standard. When the adhesive to test is rigid the specimen is longer than when testing flexible ones. Figure 18 shows the standard geometries for different adhesives.

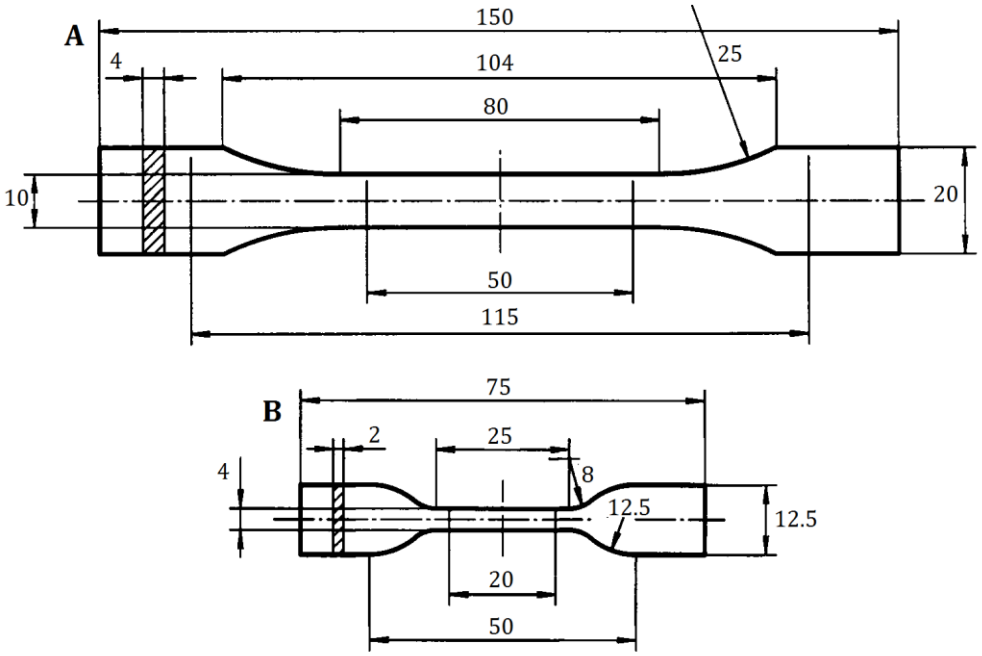

Figure 18. Tensile specimen geometry according to standard EN ISO 527-2. (A) Long specimen and (B) short specimen (dimensions in mm).

The thickness of the specimen is an important parameter to consider, since the properties obtained in the test will depend on it [25]. Unluckily, the generally used thickness of 2 mm is very far from the 0.1 or 0.2 mm thicknesses that are commonly used in adhesive joints, but thinner specimens would be difficult to test because of the high flexibility of the adhesive.

II. Test procedure and results

The specimen is submitted under a longitudinal direction load at speeds that generally are around 1 mm/min until it fails. The test can be carried out at different temperatures..

The parameters that are measured to obtain the stress-strain curve are load and displacement. The displacement can be measured by using clip gauges or strain gauges, considering that when working with high or low temperatures these devices need to be adapted to the conditions.

The typical results obtained are graphically represented in the stress-strain curve shown in Figure 19. It can be used to calculate the Young's modulus, the tensile strength and the failure strain by following the standard methods [1, 25].

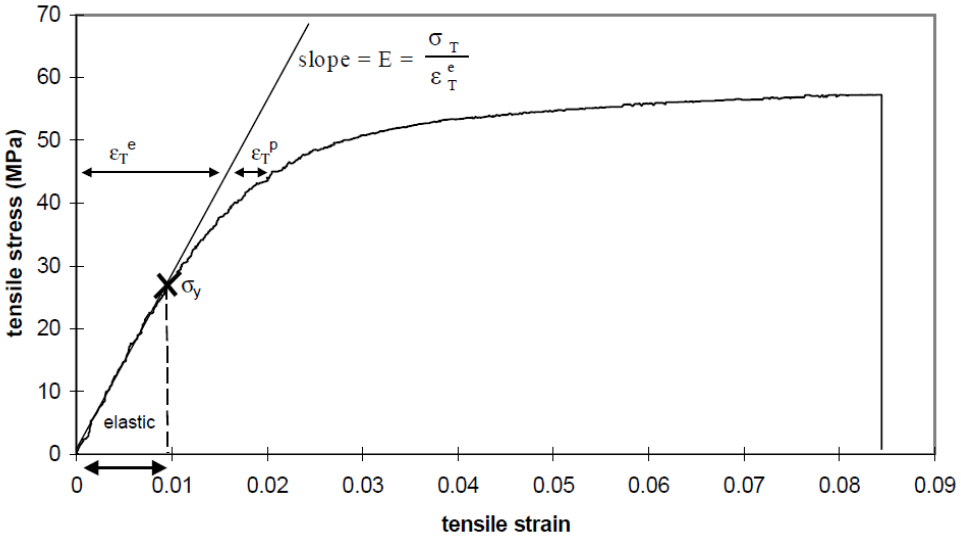

Figure 19. Common tensile stress-strain curve of an adhesive [25].

2.4.2 Quasi-static testing of Single Lap Joints

Joints with thin sheet adherends, especially SLJs, are a faithful representation of adhesive joints used in automotive and aeronautical structures. In particular, SLJ are the most simple and cheap adhesive joints to manufacture and when tested they provide accurate enough results for the *apparent* shear strength, which is the adhesive shear resistance when used in a joint [25].

The standards that describe the SLJ geometry are ASTM D 1002 and ISO 4587, although many variations can be done so that the results obtained resemble the most the real structure.

I. Specimen geometry

A SLJ basically consists in two thin sheet adherends bonded by the ends in an area called overlap (see Figure 20). Parameters such as the bondline thickness, the adherend thickness and the overlap length significantly affect the strength of the joint, which is why in many cases they are varied to compare the different results.

The width is usually around 25 mm and, depending on the type of test method, the ends of the SLJ may have thin plates welded or bonded to improve grip and make sure that the load applied is aligned with the bonding plane.

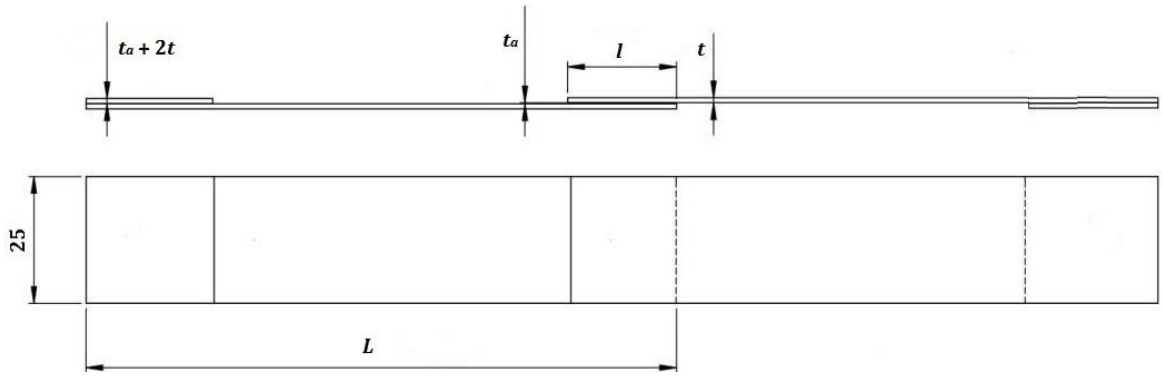

Figure 20. Single lap joint geometry.

II. Test procedure and results

As in the quasi-static bulk specimen test, the specimen is loaded in the longitudinal direction until failure, and the speed used is also generally 1 mm/min. To measure the load, a load cell is used, making sure that it is compatible with the failure load of the specimen. Meanwhile, the displacement of the cross head is being measured too, obtaining as a result the load vs. displacement curve [25].

The results for this curve can vary a lot depending on the SLJ design (materials selection and geometry) and on the testing conditions (temperature, humidity). Notwithstanding the difference between the properties obtained for the adhesive with the bulk test, this gives valuable information about the lap shear strength in real conditions [25]. Moreover, since SLJ specimens are also used in other test methods (impact tests), quasi-static results are useful to make a comparison of the properties obtained under different loading conditions.

2.4.3 Impact tests

In many situations in which adhesive joints are used, loads can be applied to them in a more abrupt way. Two kinds of impact situations are considered when it comes to test adhesive joints under impact. Firstly, in some applications in which impact loads are a

normal service condition, the main purpose is to achieve the endurance of the joint without receiving any damage.

Secondly, in situations when the impact is an exceptional case, the objective is to minimize the joint damage. Automotive industry is a clear example of these situations where structures that use adhesive bonding may undergo special conditions, as car accidents. In those cases, it is crucial making sure about how the adhesive joint is going to behave, and the best way to find it out is by conducting impact tests [23].

Different types of impact tests can be found in literature depending on how abruptly is the load applied. Due to the main objective of this thesis, this review only describes those which represent situations where impact is an exceptional case.

- *Block impact test*

The principle of this test is quite similar to the one used for Izod resilience measurement. The piece to test is a block bonded to a larger piece that is attached to the base of the machine. To apply the impact load in shear condition, a hammer-pendulum hits the little block in the side of the block which is perpendicular to the adhesive layer, so that the contact surfaces are perpendicular at the beginning of the impact. Even though the particular geometry of the bonded block that receives the impact (Figure 21) differs from real joints, it offers a large surface to make the contact and allows creating a condition of pure constant shear [1]. The standards that can be found for this test are the ASTM D950, EN 29653 and ISO 9653 [25].

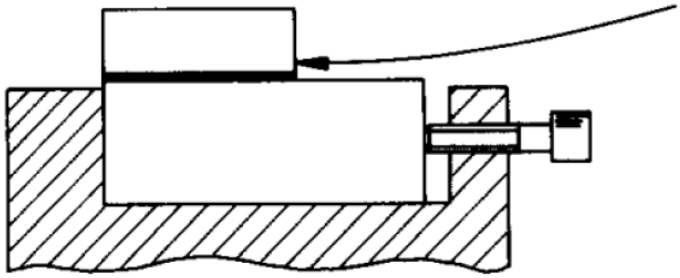

Figure 21. ASTM Block impact test [26].

However, to hit the bonded piece in a perfectly parallel direction is almost impossible and, consequently, this test carries misalignment problems that strongly affect the results obtained. Thus, this machine dependence makes this test useless when it comes

to scientifically interpret the results and compare them with other impact loaded in shear data [26].

- *Instrumented Pendulum impact test*

This test is based in the same principle as the block impact test, but Harris and Adams [24] designed a supporting device holding the specimen to solve the misalignment problems of the block impact test. The system holds the specimen with two clamps, one fixed to the machine and the other allowing movement in the longitudinal direction (see Figure 22). With this device the impact load is applied indirectly, so that it is transferred in perfect alignment to the specimen adhesive layer. Furthermore, since the specimen tested can be either a single lap joint or a bulk specimen, it is possible to compare the data obtained with scientific results from other tests.

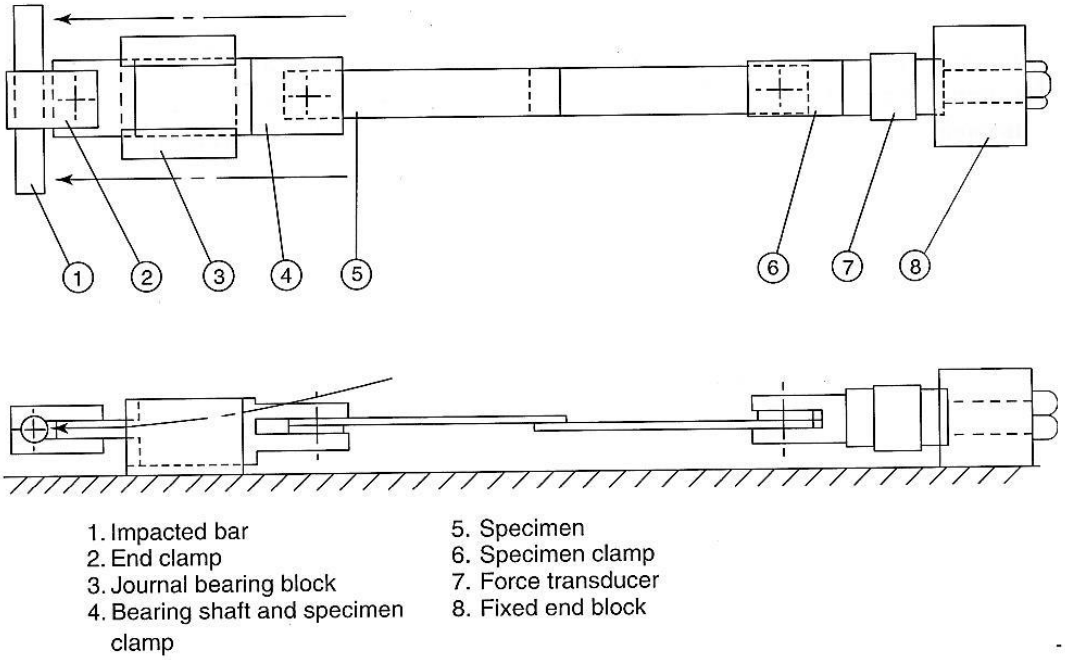

Figure 22. Instrumented pendulum test [25].

Vibration phenomena appearing in results because of the impact with the bar can be a great disadvantage, since it raises the difficulty to interpret the obtained data. Using a filter to reduce vibration is not as good solution as covering the stricken piece with a thin film, which reduces a lot the real vibrations [25].

- *Drop Weight impact test*

Although this impact test does not follow a standard regulation, it is a very reliable and commonly used method to apply abrupt load conditions in shear. As in the instrumented pendulum test, the specimen is held by a device that receives the impact, transmitting the load to the specimen. The difference lies in the hitting system.

Instead of a pendulum hammer, a mass is elevated until a certain height and then dropped guided vertically on to the test specimen. The speed and the energy applied in the impact can be easily set by changing the height or the weight, respectively. Load and displacement are measured to obtain the energy absorbed by the specimen at failure.

The configuration of the specimen used in this method depends on the device that holds the specimen, which means that many types of joints can be tested. In addition, since the falling weight either stops dead on the test specimen or destroys it completely and the load is applied unidirectional, with no preferential direction of failure, this test is a better simulation of functional impact exposures, and therefore closer to real-life conditions.

- *Impact Wedge-Peel test*

The specimen used in this test is made by two metal strips bonded together in a Y shape. A wedge loads the specimen going through the bond, separating the strips in peeling mode. Following standard ISO 11343, the strips are 90 mm long and 20 mm wide and their thickness vary from 0.6 to 1.7 mm. The bondline length is 30 mm and the not-bonded zones are clamped in a grip (Figure 23). The separating pull is applied to the shackle by a pendulum or an actuator, using a test speed around 2 or 3 m/s, depending on the material of the strips.

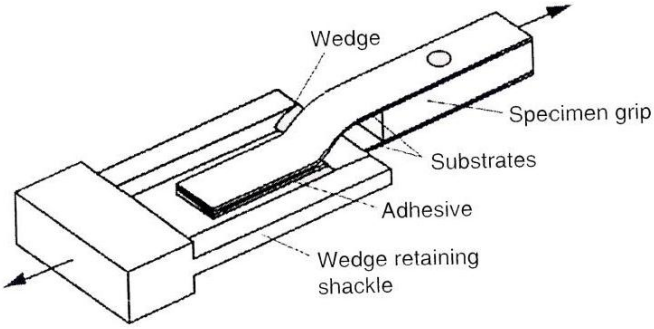

Figure 23. Wedge impact peel test specimen in the ISO 11343 standard [27].

While the test is conducted, the impact force is measured and recorded and, according to the ISO Standard, the average cleavage force can be obtained from the time history by considering the data between the 25% and 90% of the time interval in the curve. Then the energy is calculated from the area under the curve limited by these points.

When adhesives are tested with this system, two different behaviours can be observed; stable or unstable crack propagation. In the former the crack unstably grows through the adhesive layer faster than the wedge which usually happens with brittle adhesives, while in the latter the wedge sets a constant speed to the crack forcing it to grow stably [1].

- *Hopkinson Bar*

The previous impact tests methods have an important restriction regarding to the strain rate that they can provide. The Hopkinson bar device is used when higher values for strain rate are needed. The basic structure called the Split Hopkinson Pressure Bar [28] applies an impact pulse load to the specimen by holding it between two bars and striking one of them with a projectile (see Figure 24). Although this description is more suitable for testing in compression, a modification in the system can be done for testing in tension too [1].

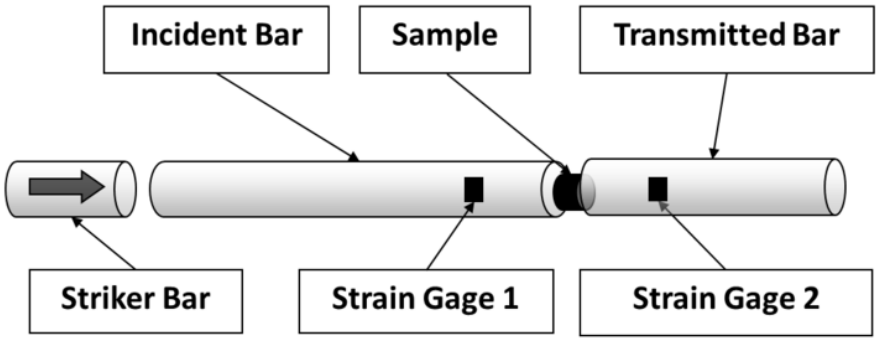

Figure 24. Schematic representation of the Split Hopkinson Pressure Bar, illustrative only [29].

Even though those are the most typical impact test configurations, a wide and almost unlimited variety of methods can be found in the literature. However, the description of all of them will be too extensive, and this selection may be an appropriate representation of the different ways to test specimens under impact loads [29].

3. Impact tests

3.1 Specimen design

3.1.1 Adhesive

The characterized adhesive was XNR6852-1, a prototype developed and supplied by NAGASE CHEMTEX® (Osaka, Japan). It is a new crash resistant epoxy adhesive with a one-part system that cures at 150 ºC for 3 h. Unlike the network structure of conventional epoxy adhesives, this adhesive has a particular linear structure that allows more freedom of movement to the chains. Other adhesives have been produced using the same technique by NAGASE CHEMTEX®, as the previous version XNR6852, which was characterized in another work [23].

During polymerization, cross-linking is generated in pure XNR 6852-1 epoxy resin, turning it into a conventional thermosetting resin. A great improvement has been achieved by introducing phenols into the pure resin, obtaining a non-cross-linking polymer. The new consecutive reaction process created polymerizes linearly the epoxy resin and the phenol, generating its new structure. Thanks to this process, the polymer obtains some similar features to thermoplastic polymers [23, 30].

The adhesive mechanical properties at room and high temperature summarized in Table 3 were obtained by performing tensile bulk tests. An extended explanation of the procedure and the experimental results can be found in section 4.

Table 3. Properties of the adhesive at different temperatures obtained in the bulk tests.

	Tensile strength (MPa)	**Young modulus's (MPa)**	**Strain to failure (%)**
XNR6852-1 23 ºC	56.21 ± 2.01	2187.4 ± 93.4	21.14 ± 5.91
XNR6852-1 80 ºC	10.88 ± 0.47	278.73 ± 2.41	100.9

3.1.2 Adherends

The adherends material used to manufacture the SLJ was mild steel (DIN St33) because of its strong presence in the automotive industry for car body shells. Due to the low strength of this material it was expected to obtain adherend yielding when tested at room temperature, so that the effect on the joint strength could be studied.

To know the exactly properties of this steel a tensile test was conducted (also explained in section 4), obtaining results showed below in Table 4.

Table 4. Properties of the steel used for the SLJ adherends.

	Young's modulus (GPa)	Yield strength (MPa)	Tensile strength (MPa)	Strain to failure (%)
DIN St33	205	176.9 ± 1.5	271.1 ± 1.6	41.1 ± 1.7

3.1.3 Specimen manufacture

Two groups of SLJs were used, with the only difference between them lying in the bondline thickness, which was 0.2 mm and 0.4 mm. Thus, later conclusions could be drawn about the effect of thickness under impact load. The mild steel adherends thickness was 1 mm, the overlap length was 12.5 mm and the width was 25 mm. The whole SLJ geometry is given in Figure 25. This geometry was chosen because it is usually used in automotive industry and will therefore allow comparison with other academic work. Moreover, it is representative of a structural part.

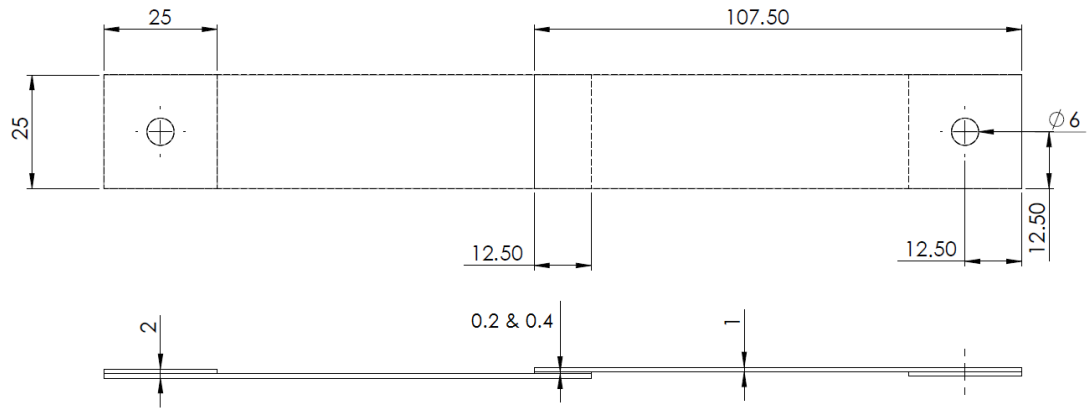

Figure 25. SLJ geometry used in the impact tests (dimensions in mm).

The manufacture process began by sandblasting and degreasing with acetone the substrates surface corresponding to the overlap. Then, the substrates were placed in a mold for correct alignment (Figure 26) with the proper spacers for adhesive thickness control. The closed mold was left under 2 MPa pressure for 3 h at 150 ºC in an hydraulic hot plates press, removing any excess adhesive in the SLJs at the end of the curing process.

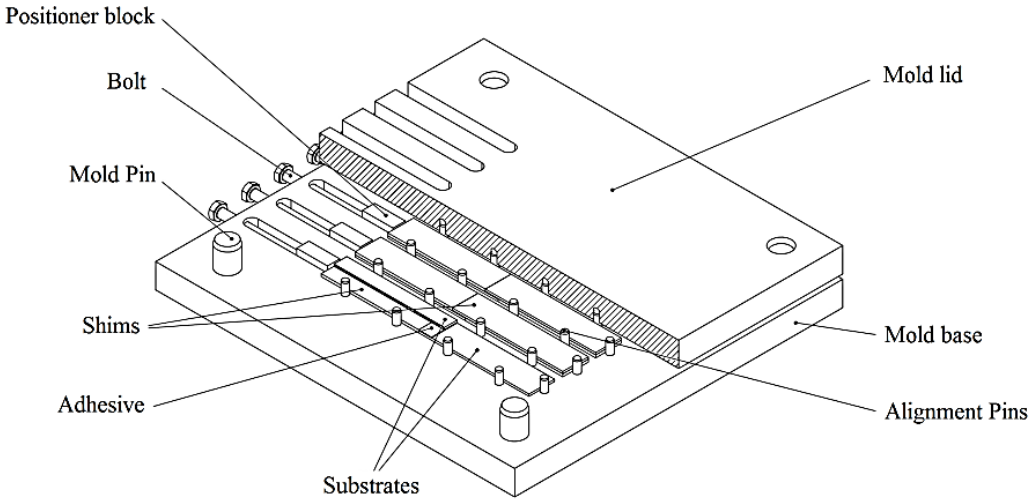

Figure 26. Schematic representation of the mold for SLJ specimens [30].

Once the curing process was over and the excess adhesive was removed, two steel plates were welded at the ends of the specimen to improve grip in the impact machine. The final step was to drill two holes at the ends to allow the assembling of the specimen to the machine holding device. The final specimen obtained is shown in Figure 27.

Figure 27. SLJ specimen manufactured for impact tests.

3.2 Room temperature impact tests

3.2.1 Tests procedure

The impact tests were conducted in the machine Rosand® Instrumented Falling weight impact tester, type 5 H.V. (Stourbridge, West Midlands, U.K.). This machine drops a mass guided from certain high until it impacts on the device that holds the specimen. The energy applied in the impact is controlled by the weight of the falling mass, and the speed can be set by the height.

To start explaining the systems designed and used to reach the high and low temperatures, it is essential to describe the holding device in first place. Figure 28 show the holding device used for SLJ in impact tests.

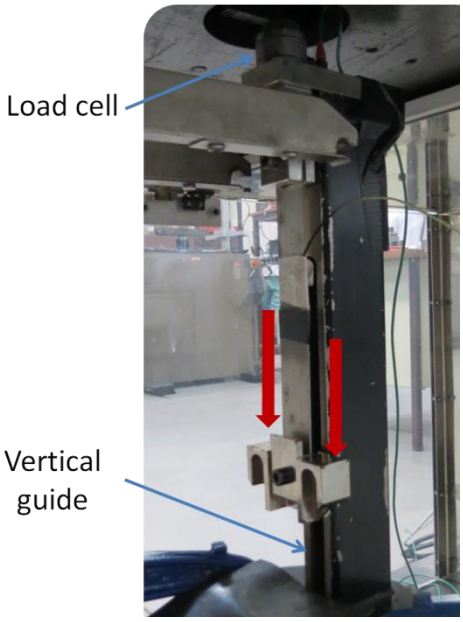

Figure 28. SLJ assembled with the holding device.

When common tests at room temperature are performed with this machine, the specimen needs to be assembled to this device which receives and transmits the impact load. This process takes some time, which is an important thing to consider when it comes to perform the high and low temperature tests. Once everything is properly set, the weight is dropped and it falls on the lower piece attached to the specimen. The load was vertically transmitted to the SLJ thanks to the vertical guide. A load cell on the top of this holding device was used to measure load and time and thus the results of the test were obtained.

The room temperature tests were performed following the procedure explained in the past section. The holding device was calibrated to make sure that the load was correctly aligned when applied. After assembling the specimen, the mass was set to provide an impact energy of 320 J, which was the maximum capacity available with the specified machine. The height was set to give an impact speed of 4.55 m/s. For each adhesive thickness, three specimens were tested keeping the same conditions.

3.2.2 Results

In this section the results of energy absorbed, failure load, elongation and failure mode are shown. The respective analysis of these results is explained in a later section, so that a comparison with the quasi-static tests and the prediction is done, obtaining the final conclusions.

Results of load vs. displacement curve were displayed by the software of the impact machine and the energy absorbed was automatically calculated by the area below that curve. The average load failure was calculated as the energy absorbed divided by the elongation at failure, since the maximum failure load showed too much scattering due to the oscillating shape of the curve (see Figure 29). Table 5 summarizes the average plus std. deviation results of impact tests at room temperature for both 0.2 and 0.4 mm bondline thicknesses.

Table 5. Impact results at room temperature.

	Energy absorbed (J)	**Max. Failure Load (kN)**	**Avg. Failure Load (kN)**	**Elongation (mm)**
0.2 mm at 23 ºC (not broken)	245.5 ± 31.2	7.36 ± 0.02	3.91 ± 0.75	63.1 ± 4.1
0.2 mm at 23 ºC	197.40	7.85	5.15	38.30
0.4 mm at 23 ºC	126.24 ± 17.08	7.17 ± 0.04	4.31 ± 0.52	29.25 ± 1.51

As a result of the high ductility of the steel adherends and the adhesive strength, only one of the three specimens tested with 0.2 mm adhesive thickness broke at room temperature, even though the energy applied was the maximum available. Although results of specimens that did not break are more representative of the adhesive strength, they cannot be compared with previous academic work. For this reason, only the results of the broken specimen were considered, which is why no standard deviation appears in this case. The load vs. Elongation curves are represented graphically in Figure 29, comparing the specimens with different adhesive thicknesses.

Figure 30 shows the fracture mode of the 0.2 mm adhesive thickness SLJ which broke, and two other SLJ that did not break with the same energy applied. A cohesive fracture was perceived in the adhesive with high adherend yielding in the broken specimen. The specimens that did not break showed also high deformation in the adherends and a little crack appeared in the adhesive, meaning that the joints were about to break (see Figure 31). For SLJs with 0.4 mm adhesive thickness the fracture mode was the same as the one shown in Figure 30. It can be observed that with a thicker bondline the joint strength decreased and, as a result, all the specimens broke, experimenting the same high yielding in the adherends.

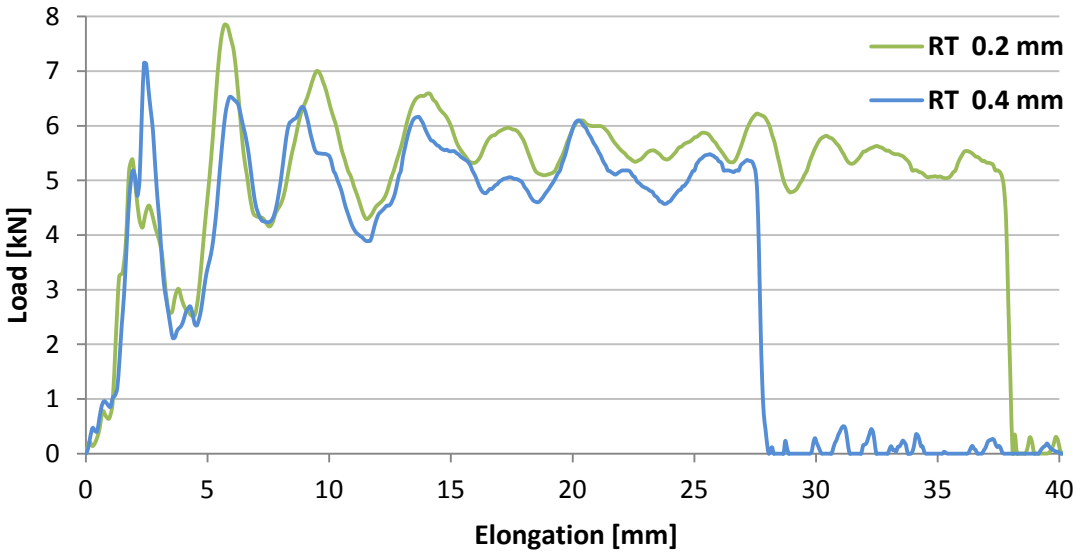

Figure 29. Load vs. elongation curves for room temperature impact tests.

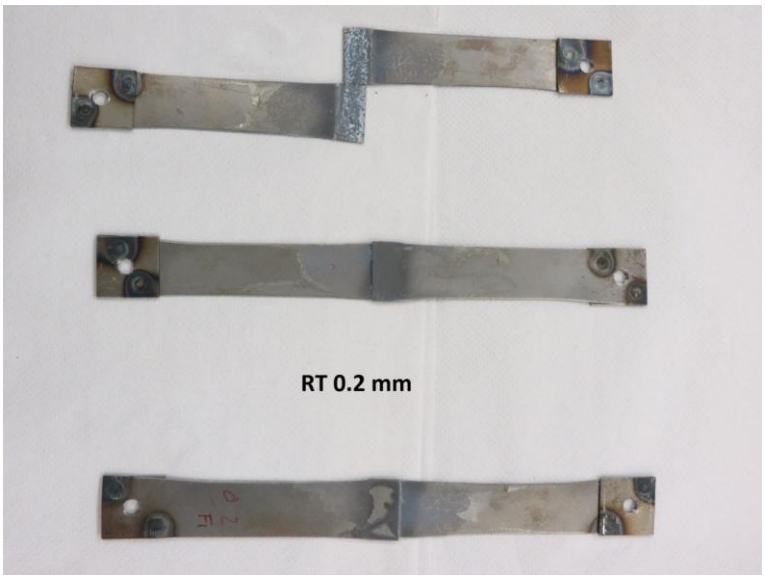

Figure 30. Failure mode for impact tests at room temperature in 0.2 mm adhesive thickness SLJ.

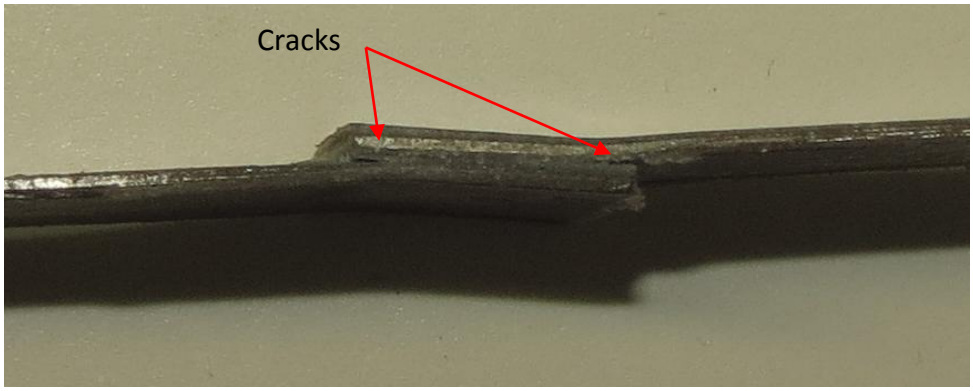

Figure 31. Adhesive crack in a tested SLJ of 0.2 mm thickness that did not break.

3.3 High temperature impact tests

3.3.1 Heating system design

The bonded part of the specimen needed to be tested at 80 ºC. The solution thought to reach this temperature and also to satisfy the requirements mentioned before was to use heating through electromagnetic induction. The reason why it was chosen is that it has been already successfully used in many other researches [31, 32] to obtain a homogeneous and constant temperature over a specific area.

The basic principle consists in an electric current circulating through a coil made of conductive material that generates a magnetic field. The highest intensity of the magnetic field appears in the coil core and it depends on the strength of the excitation current and the number of turns of the induction coil. When a ferromagnetic material is placed inside the magnetic field, electric currents are induced in the material, called Foucault currents. This currents move the particles of the materials generating heat by Joule effect (see Figure 32) [33].

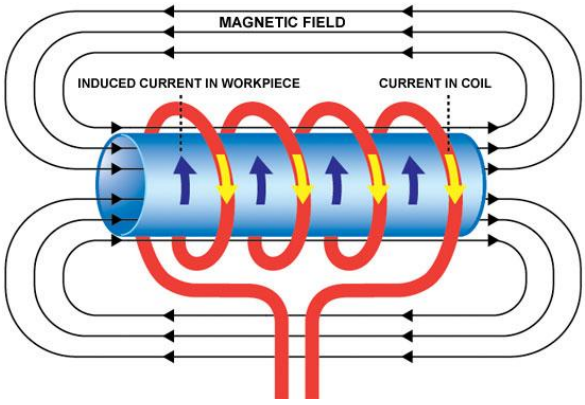

Figure 32. Basic principle of electromagnetic induction heating [34].

This particular solution has many advantages referring to the drop weight impact test of adhesive joints. One of the most important is the adaptability to many applications, since the range of possibilities for the induction coil geometry is wide. The area is heated homogeneously and the temperature can be easily controlled by varying the intensity of current. Furthermore, there is no physical contact with the specimen and the heating process is cheap and fast [35]. The only disadvantage that entails this solution is that a thermocouple cannot be used to check the temperature because of the interferences with the magnetic fields.

To build an induction heating systems, three components were required (see Figure 33). The first element is the power source (Figure 33-1), which receives the AC, rectifies and regulates it feeding the frequency converter that enables the generation of the magnetic field. Frequency can be varied depending on the piece to heat. For thick materials, low frequencies (5 – 30 kHz) are recommended while for thin pieces higher frequencies are necessary (100 – 400 kHz). The second element is the heating station (Figure 33-2), and its role is to adjust the frequency or the voltage for the application and to refrigerate the induction coil using a water circuit. The last one is the induction coil (Figure 33-3). It is usually made of copper and hollow inside so that water can circulate through it [33].

Figure 33. Induction heating system used for the high temperature impact tests.

Two geometries were selected to manufacture the induction coil due to the particular geometry of the whole specimen plus holding device. The induction coil had to be inserted in the little space between the specimen and the device and easily removed later, avoiding contact in any case.

Figure 34. Induction coils manufactured (pancake shape at left and U-shape at right).

Two induction coils were manufactured with a 'pancake shape' and 'U-shape' and tested later (see Figure 34). Both of them reached successfully the 80 ºC with a homogeneous heating, but the 'pancake shape' was discarded because it was impossible to introduce it in the holding device without making physical contact. Figure 35 shows the heating of the assembled SLJ by using the 'U-shape' induction coil.

Figure 35. Heating of the specimen for the impact test at high temperature.

3.3.2 High temperature tests procedure

The procedure to perform the impact tests at high temperature was simple. Once the holding device had been properly calibrated and the specimen assembled, the mass was set at the right height to provide an impact speed of 4.47 m/s and 150 J. In this case, lower energy was applied because the joints were expected to break easier. Then the heating system was turned on until the temperature was a few degrees above 80 ºC, when the heating station was carefully removed. Finally the weight was dropped a few seconds after the removing of the coil, so that the temperature was approximately 80 ºC.

To check the temperature while this procedure was being carried, a thermographic camera was used. It provided infrared spectrum images of the temperature, proving that the temperature was homogeneous over the overlap (see Figure 36). To avoid reflections changing the emissivity of the steel, a black adhesive tape covered the overlap.

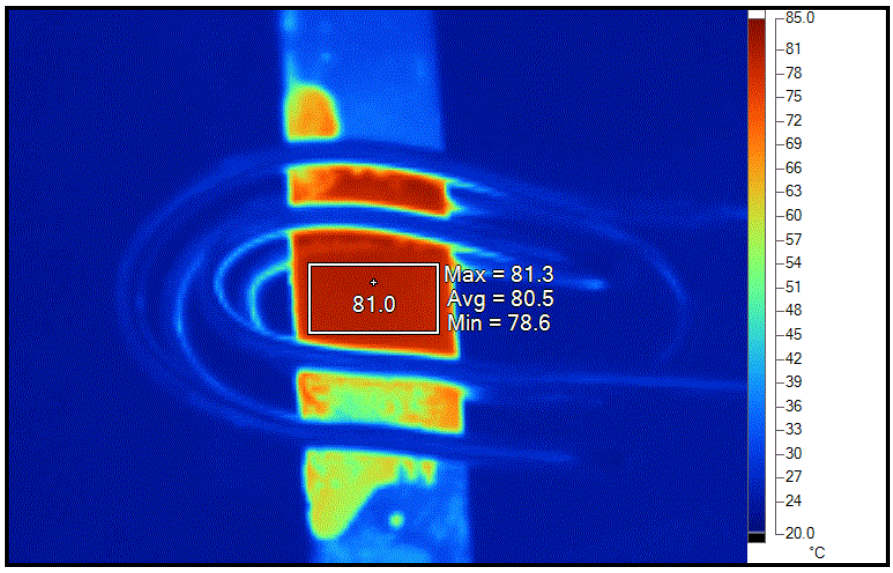

Figure 36. Infrared spectrum of the induction heating in the overlap.

3.3.3 Experimental results

Table 6 summarizes the results of impact tests at 80 ºC for both bondline thicknesses.

Table 6. Impact results at high temperature.

	Energy absorbed (J)	Max. Failure Load (kN)	Avg. Failure Load (kN)	Elongation (mm)
0.2 mm at 80 ºC	42.33 ± 13.42	4.73 ± 1.05	2.60 ± 0.41	15.75 ± 2.60
0.4 mm at 80 ºC	20.03 ± 3.23	4.79 ± 0.45	2.29 ± 0.22	8.67 ± 0.66

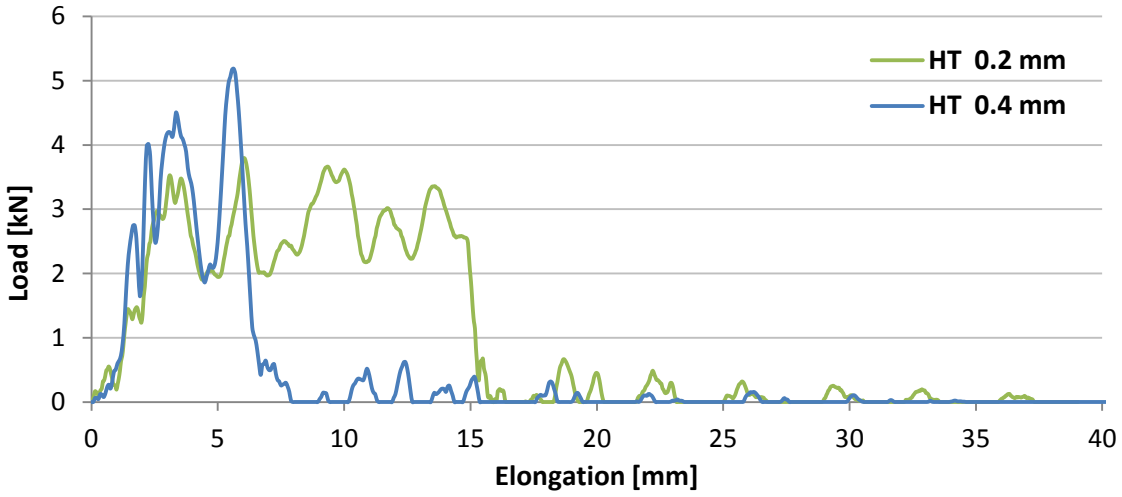

Figure 37. Typical load vs. elongation curves for high temperature impact tests.

Figure 37 shows typical load vs. elongation curves obtained in high temperature impact tests for the two thicknesses. The fracture mode of the SLJs tested under impact at 80 ºC is displayed in Figure 38 and Figure 39. In both SLJs with different adhesive thicknesses, a fracture surface of the adhesive typical from a ductile behaviour can be observed, as expected when the adhesive works at high temperatures. Unlike in room temperature fracture mode, in this case no significant adherend yielding was observed, which implies that the joint failed due to the adhesive.

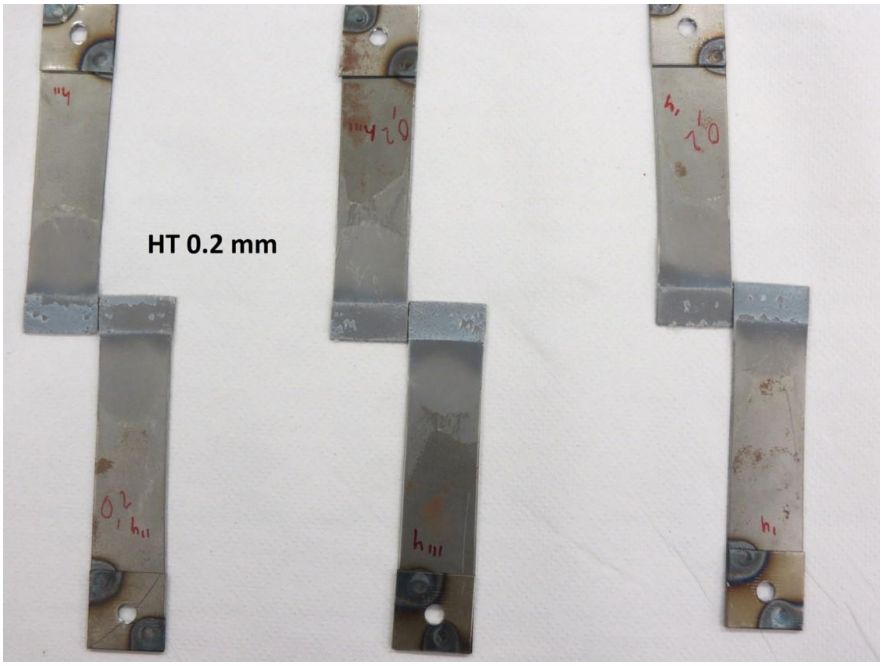

Figure 38. Failure mode for impact tests at +80 ºC in 0.2 mm adhesive thickness SLJs.

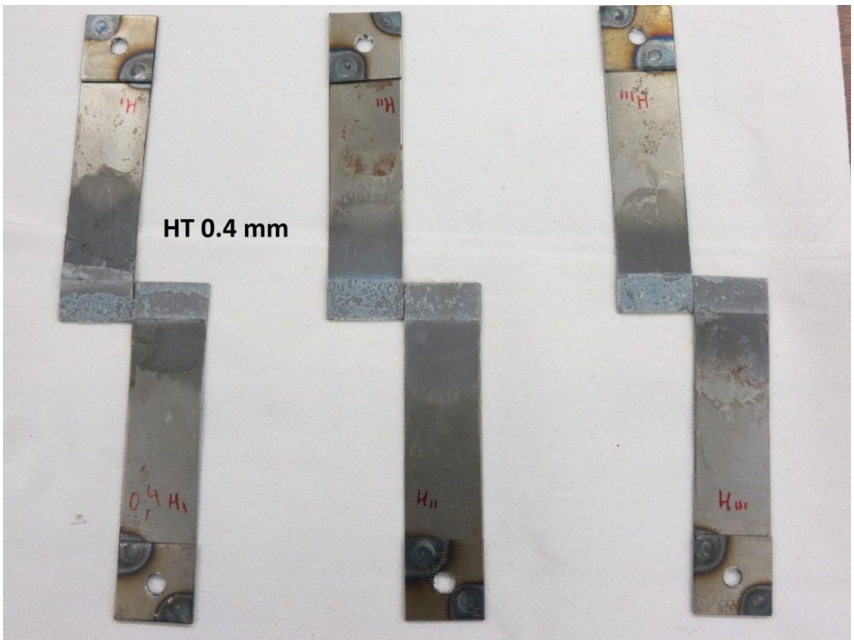

Figure 39. Failure mode for impact tests at +80 ºC in 0.4 mm adhesive thickness SLJs.

3.4 Low temperature impact tests

3.4.1 Cooling system design: failed attempts

To reach the required temperature of -20 ºC the first solution thought was to develop a cooling system using dry ice. The idea consisted in manufacturing an isolating chamber containing the specimen overlap in conjunction with the dry ice. The atmosphere inside the box would be cooled and the temperature of the specimen would decrease by convective heat transfer. Dry ice is the common name for frozen carbon dioxide. It stays at the temperature of -78.5 ºC and changes directly from solid to gas (sublimation). Due to its ease to be used and manipulated for freezing, it is widely used in recent years in many applications.

The designed isolating chamber in this first solution contained only the overlap part of the specimen. The intention was to avoid as many leaks as possible considering the geometry of the assembled holding device with the specimen. Furthermore, the load cell was kept isolated from the cold. If it were otherwise, the measures would have been wrong.

The chamber was manufactured using foam for the structure as an isolating material and the different parts were bonded with a silicone glue to fill the gaps between the pieces. A wall made of aluminium grill kept the dry ice separated from the specimen, and a plastic shape was bonded in each part to hold the dry ice inside when the two parts were separated. Figure 40 shows the built chamber opened with a SLJ specimen.

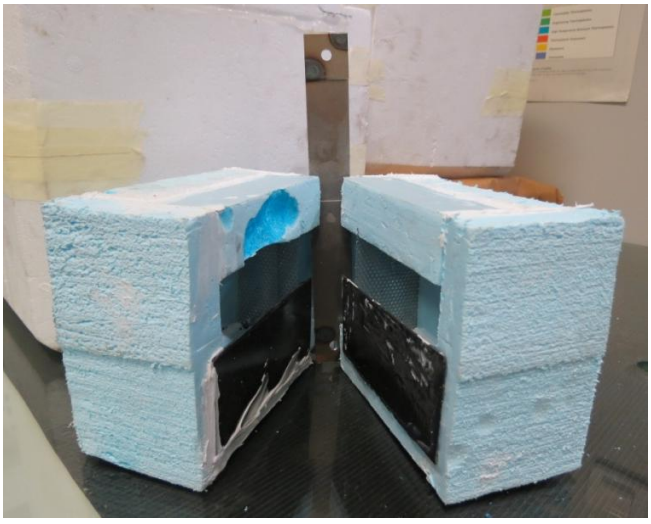

Figure 40. First isolating chamber manufactured.

The isolating chamber was tested to check if the specimen overlap could reach the temperature of -20 ºC. To measure the temperature, a thermocouple was used attached to the specimen while the box was closed (see Figure 41).

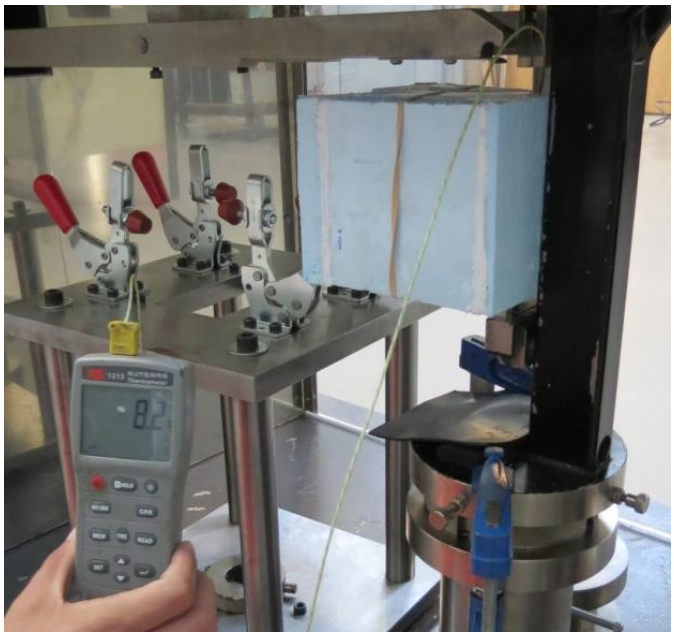

Figure 41. Testing the first isolating chamber manufactured.

Unfortunately, this first solution did not work, since the lowest temperature achieved was -5 ºC. Although the chamber had many leaks, it was deduced that the main cause of the failure was the little space to contain the dry ice. The amount of dry ice needed to cool until the required temperature was not enough and therefore it was necessary to build a bigger box.

The second solution consisted on manufacturing a bigger isolating chamber containing the whole holding device except the load cell. Liquid nitrogen was used in this case instead of dry ice. The liquid nitrogen is pure nitrogen that remains in this state at a temperature lower than 195.8 ºC. It is also widely used as the dry ice but, due to its higher power of cooling, it is difficult to manipulate.

The structure of the bigger isolating chamber was practically the same as the previous one, but the material used to build it was extended polystyrene. The liquid was placed inside the box on a aluminium foil cover, so that the structure would not be damaged. This second chamber is illustrated in Figure 42.

Figure 42. Second isolating chamber manufactured.

When this second cooling system was tested, the temperature inside the box decreased too fast and the specimen reached temperatures far below the -20 ºC. Since temperature could not be controlled properly, this solution was also discarded.

3.4.2 Cooling system final design and test procedure

Since the idea of building an isolating chamber did not work out, the approach of the design for the cooling system was changed. The last and successful solution was based on using also liquid nitrogen. In this case the nitrogen liquid was contained inside a bottle at a certain pressure and it was manually sprayed using a dispenser over the specimen overlap (see Figure 43).

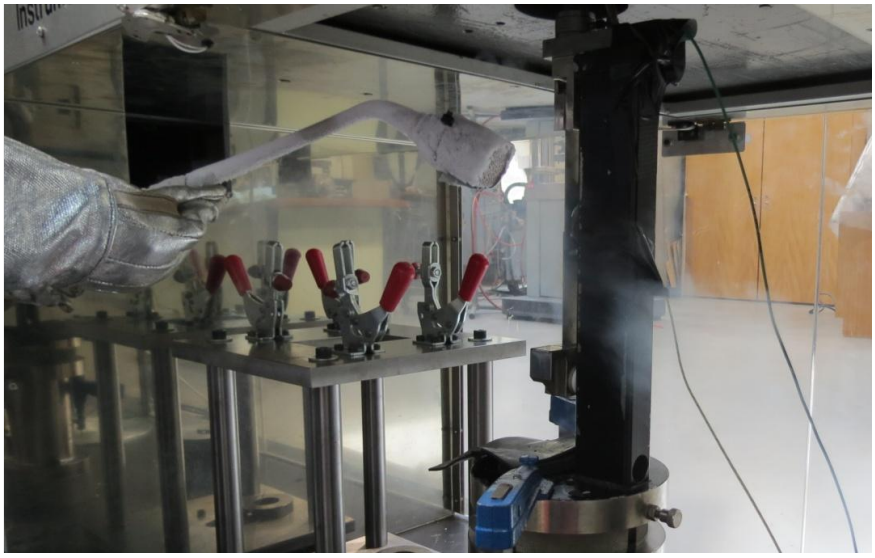

Figure 43. Cooling system using a nitrogen gas sprayer.

In this case, it was possible to use a thermographic camera to control the temperature in the overlap. The infrared spectrum displayed in Figure 44 shows that the temperature was approximately around -20 ºC. However, due to the reflections in the metallic surface, the spectrum did not provide a homogeneous distribution of the temperature. The black adhesive tape could not be used this time in order to allow the nitrogen gas to cool the specimen surface, which made impossible to obtain a constant emissivity over the specimen. Despite this, a thermocouple was attached behind the specimen to make sure that the overlap was at the right temperature.

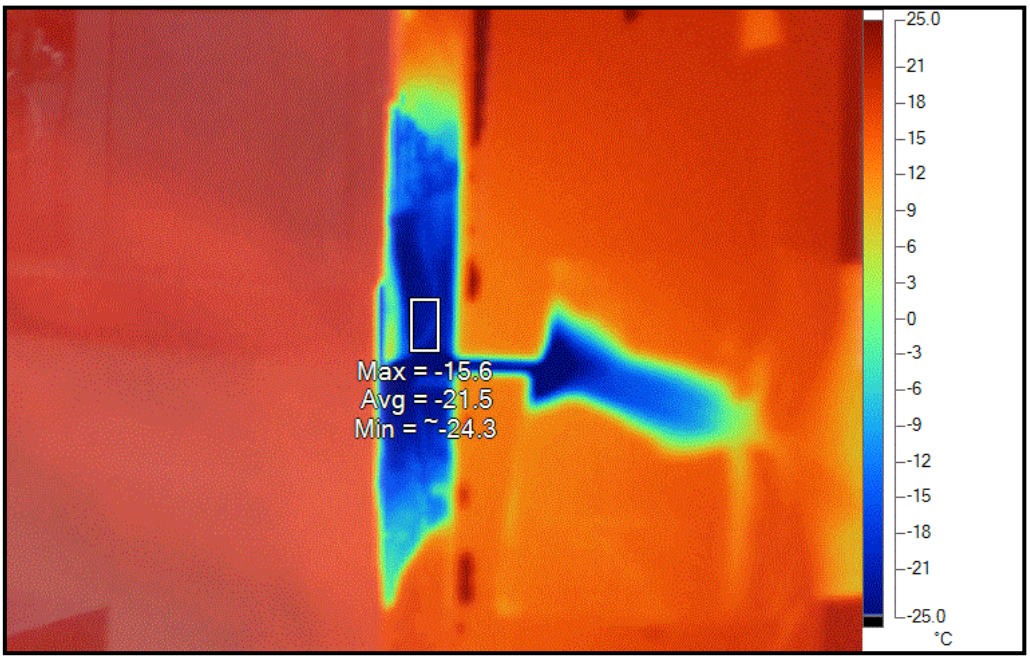

Figure 44. Infrared spectrum of the cooling system.

This last solution was a high improvement in regard to the previous ones, since it could reach the -20 ºC much faster than using dry ice and the control of the temperature was easier than using liquid nitrogen. However, comparing to the heating system it had some disadvantages. It did not cool the specimen overlap from inside, as the electromagnetic induction, but from one surface side, and it had to be carefully sprayed in order to not interfere with the load cell.

The impact tests at low temperature using this system were conducted as the high temperature tests. The energy applied was 150 J and the impact speed provided was 4.47 m/s, so that the conditions of the high temperature impact tests were kept. The specimens were cooled until a few degrees less than -20 ºC so after some seconds, at the moment of the impact, the SLJ was at the right temperature.

3.4.3 Experimental results

The results obtained in low temperature impact tests are displayed in Table 7.

Table 7. Impact results at low temperature.

	Energy absorbed (J)	Max. Failure Load (kN)	Avg. Failure Load (kN)	Elongation (mm)
0.2 mm at -20 ºC	9.45 ± 0.78	7.06 ± 0.98	2.39 ± 0.30	3.97 ± 0.21
0.4 mm at -20 ºC	5.34 ± 1.65	5.00 ± 1.72	1.53 ± 0.33	3.40 ± 0.38

Typical load vs. displacement curves are shown in Figure 45. In this case the displacement is very short and, as a consequence, the maximum failure load is defined in one only peak. Thus, the average failure load value is not as representative as in the other cases.

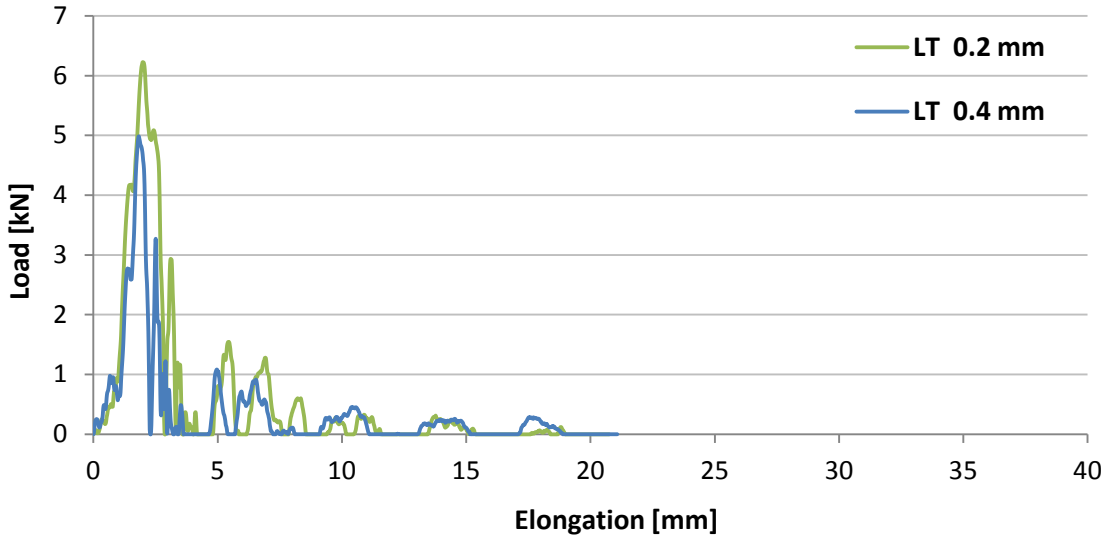

Figure 45. Typical load vs. elongation curves for low temperature impact tests.

The fracture mode of SLJs tested under impact at -20 ºC is shown in Figure 46 and Figure 47. Due to the brittle behaviour of the adhesive at this temperature, the adherends had very little yielding and the joint failed almost only by the adhesive. In both cases with different adhesive thickness, cohesive failure in the adhesive was detected with a typical brittle fracture.

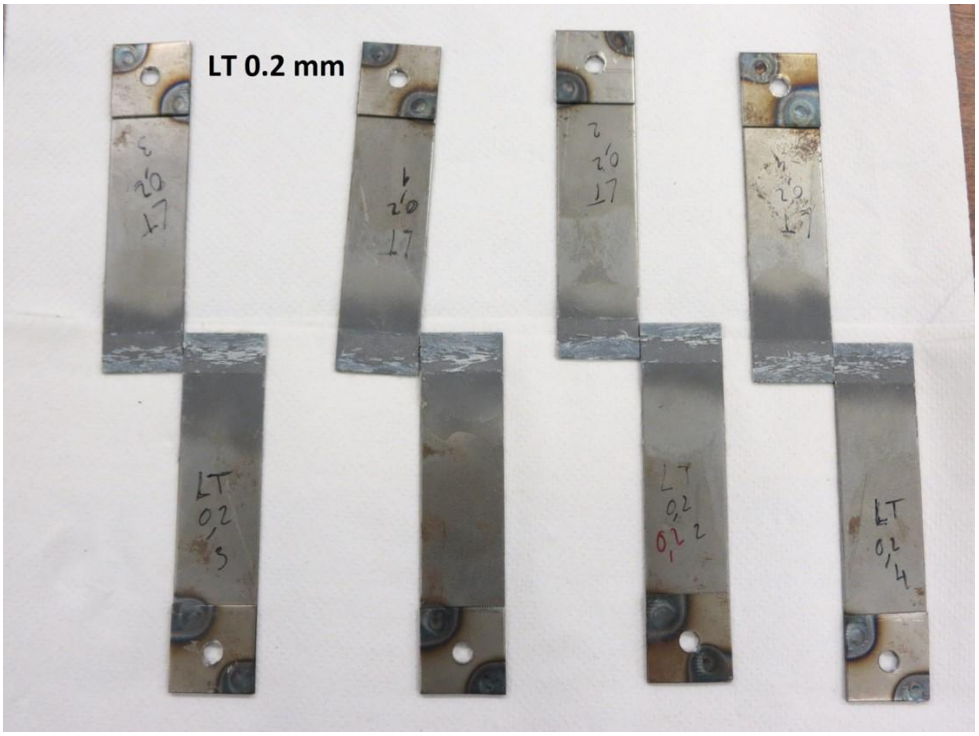

Figure 46. Failure mode for impact tests at -20 ºC in 0.2 mm adhesive thickness SLJs.

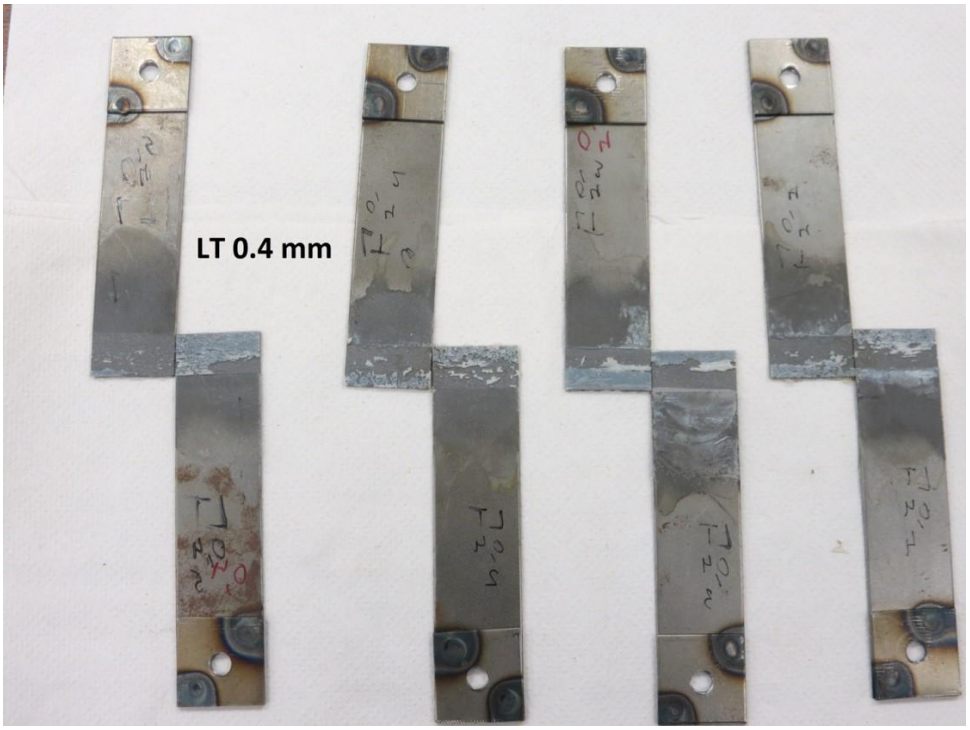

Figure 47. Failure mode for impact tests at -20 ºC in 0.4 mm adhesive thickness SLJs.

4. Tensile Tests

4.1 Steel adherends

To analyze the results obtained in the impact tests, it is essential to know exactly the properties of the materials used for the specimens. The substrates used to manufacture SLJs were made of mild steel. Although the provider of the steel was the same as in the study of the previous version of the adhesive under impact [23], the behaviour observed in the impact tests results led to suppose that the properties might not be the same. For this reason, tensile tests of the steel were conducted in order to obtain its real properties.

4.1.1 Specimen geometry

The tested steel specimen was a dog-bone sheet of 1 mm thickness and the geometry, given in Figure 48, followed ASTM E 8M subsize specimen standard.

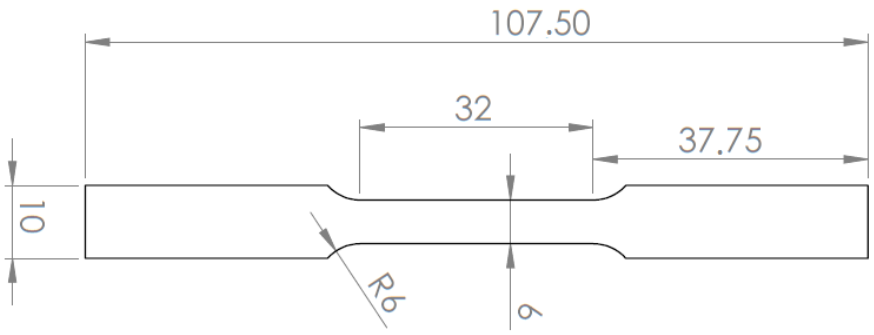

Figure 48. Dog-bone sheet specimen tested following ASTM E 8M standard (dimensions in mm).

4.1.2 Test procedure and results

The specimens were tested by the universal test machine INSTRON® model 3367 (Norwood, Massachusetts, USA) with a capacity of 30 kN. The tests were performed at room temperature with a constant displacement rate of 1 mm/min. To measure the displacement, an extensometer was used and loads and displacements were recorded until failure.

Due to the high adherend yielding appeared in the impact tests, the value of the tensile strength should be considered instead of the yield strength for failure load prediction, since it is more representative of the failure of the steel. Moreover, since the experimental results showed that the specimen dimensions experienced substantial changes while deforming, the engineering curve should be interpreted with caution [36]. True stress and true strain were also calculated to obtain a more reliable value of the tensile strength of the steel. Comparison between the engineering and the true curve is represented in Figure 49.

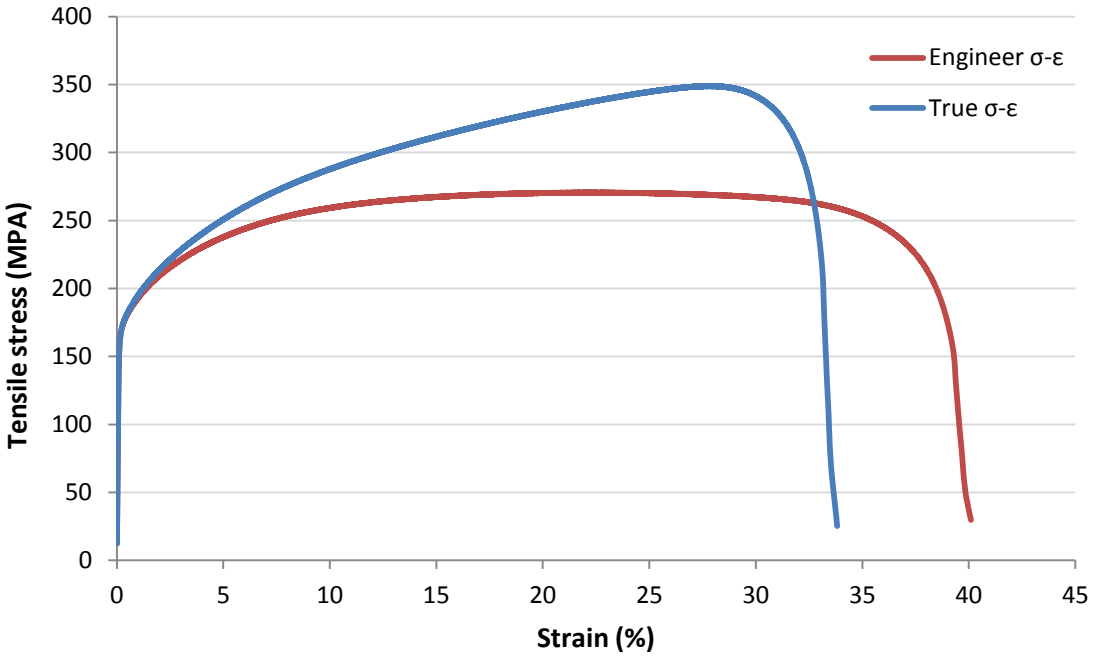

Figure 49.True and engineering stress-strain curves obtained from the steel tests.

The mechanical properties were calculated from the stress-strain curves and the results are summarized in Table 8.

Table 8. Mechanical properties of the DIN St33 steel obtained in tensile tests.

	Young's modulus (GPa)	Yield strength (MPa)	Tensile strength (MPa)	Strain to failure (%)
Eng. σ-ε	205	176.9 ± 1.5	271.5 ± 1.6	41.1 ± 1.7
True σ-ε	205	177.9 ± 1.1	350.2 ± 6	34.4 ± 1.2

Young's modulus value could not be accurately calculated from the stress-strain curve and the catalogued value was considered correct, since there is no significant difference between different types of steel. Although the results for the yield and tensile strength were very similar to the values shown in the previous work (see Table 9), the steel used in this case resulted much more ductile, which explains why the adherends of the SLJ with 0.2 mm adhesive thickness did not break at room temperature, even when the impact test conditions were the same [23, 30].

Table 9. Mechanical properties of the substrates for the standard steel used in previous work [29].

	Young's modulus (GPa)	Yield strength (MPa)	Tensile strength (MPa)	Strain to failure (%)
Prev. DIN St33	205	183.8	288	17.6

The three tested steel specimens showed a ductile fracture (see Figure 50). Deformation was essentially uniform throughout the specimen until necking formation appeared. Due to the dimensions of these specimens, the fracture happened soon after the necking.

Figure 50. Fracture mode of the steel specimens tested.

Although usually the true tensile strength is not a direct measure of the material strength because of its dependence on the geometry of the specimen [36], since the adherends showed such a high yielding in the impact tests it can be used to approximately predict the joint strength.

4.2 Adhesive

Although testing adhesive joints give a more accurate characterization about how the adhesive behaves in real situations, bulk tensile tests are a good method to obtain the mechanical properties of the adhesive with no influence of the properties of the adherends. Then, it is possible to understand how an adhesive responds under different conditions when used in a joint by performing bulk tests under these conditions.

In this case, bulk adhesive tests were performed to understand why under impact load at room temperature the strength of the joint lied on the adherends, while at high and low temperatures the failure was induced by the adhesive. Unluckily, the lack of means and time made unfeasible to perform the bulk tests at low temperature, which is why only room temperature and high temperature are described in this section.

4.2.1 Bulk tests at room temperature

The adhesive tested was the same as the one used for the impact tests, the XNR6852-1 supplied by NAGASE CHEMTEX® (Osaka, Japan). The specimens were manufactured following the French standard NF T 76-142, which consists on curing the adhesive between steel plates of a mold with a silicone rubber frame, used to avoid the adhesive from flowing out (see Figure 51).

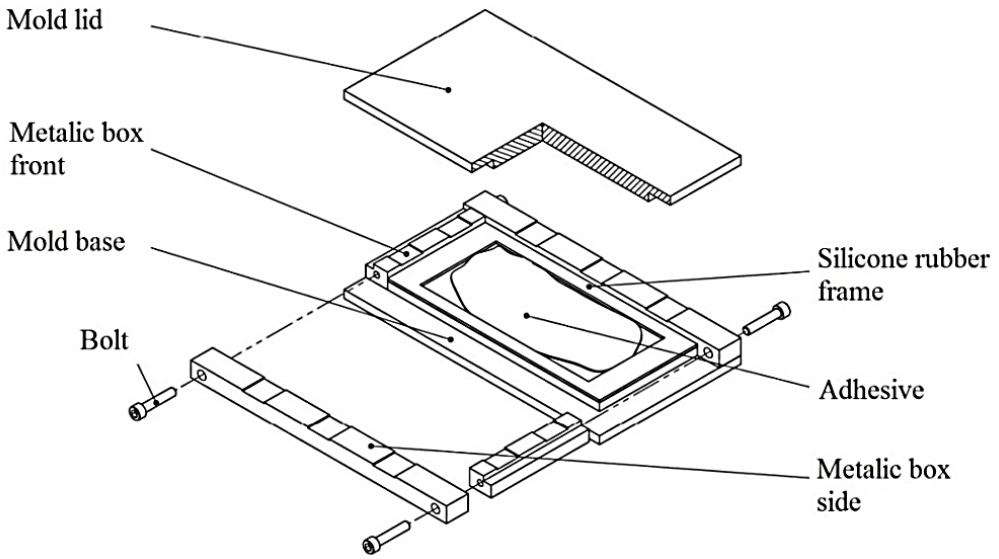

Figure 51. Scheme of the mold used to manufacture plate specimens [30].

The specimens were machined from the bulk plates to obtain the final geometry shown in Figure 52. Although it did not follow a standard geometry, it has been demonstrated in previous work that it kept the same elastic properties as with standard specimens while the productivity was improved [30].

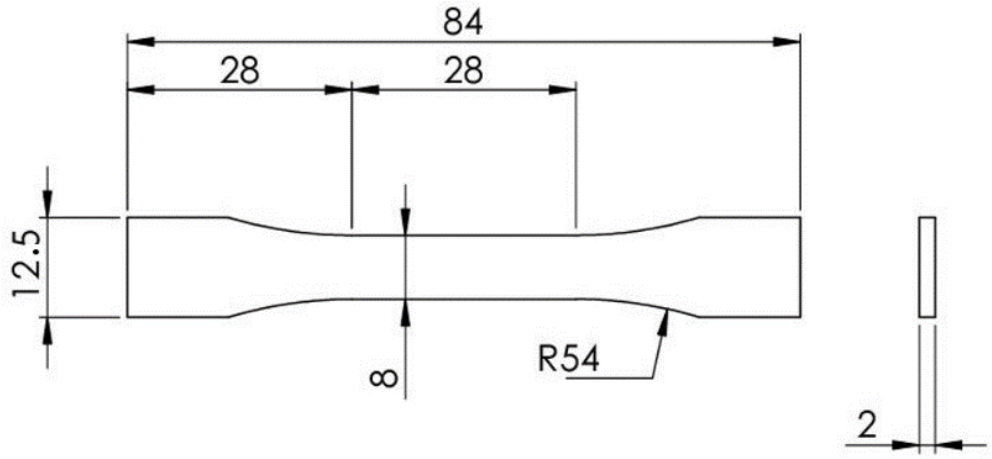

Figure 52. Short specimen geometry used in previous work [30].

The bulk tensile tests were performed using the universal test machine INSTRON® model 3367 (Norwood, Massachusetts, USA) with a capacity of 30 kN and a constant separating speed of 1 mm/min. To measure the displacement two marks were drawn on each specimen and a camera was used to make 5 seconds time-lapse. Then a software was used to automatically analyze the pictures and convert them into strain data, making each value correspond to its respective stress value. The results of the tests are summarized in Table 10, comparing them with the mechanical properties of the previous version of the adhesive [23]. Although the geometry used for the specimens gives correct values of the elastic properties of the adhesive, the ductility value is not comparable to that calculated for the previous adhesive.

Table 10. Mechanical properties of the adhesive at RT compared with the previous version [23].

	Tensile strength (MPa)	**Young's modulus (MPa)**	**Strain to failure (%)**
XNR6852-1	56.21 ± 2.01	2187.4 ± 93.4	21.14 ± 5.91
XNR6852	59.9 ± 0.84	1176.3 ± 39.9	100.7 ± 25.52

Figure 53 shows the stress-strain curve obtained for the XNR6852-1 at room temperature. The shape of a typical tough rubbery polymer is observed without any necking such as the typical thermoplastic curve showed by the previous adhesive.

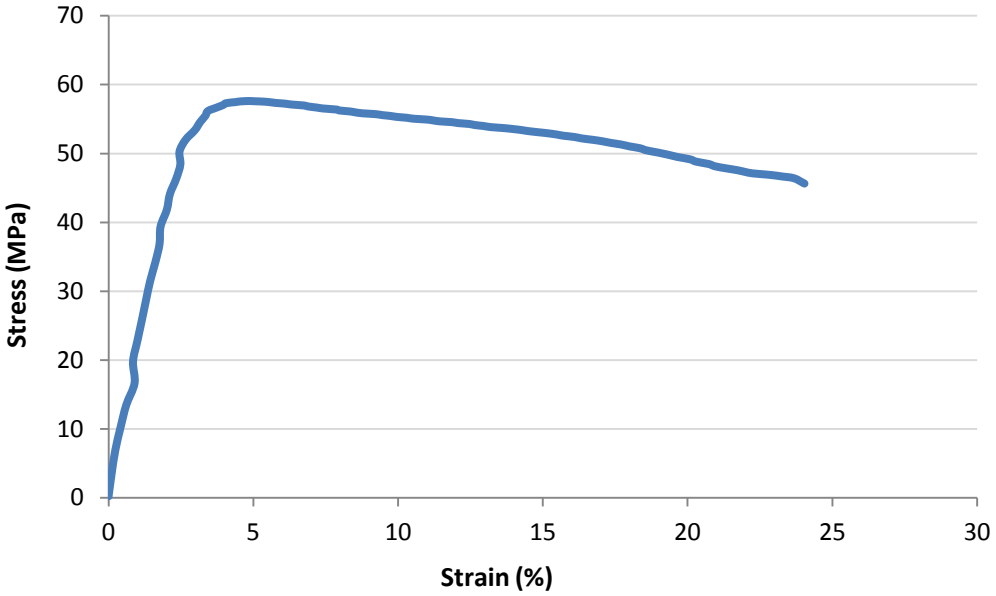

Figure 53. Stress-strain curve of XNR6852-1 obtained in the bulk tests at RT.

The fracture mode displayed in Figure 54 of one of the specimens shows that the adhesive had some ductile deformation before failure but, as noticed in the curve, the necking is not as significant as in the previous version.

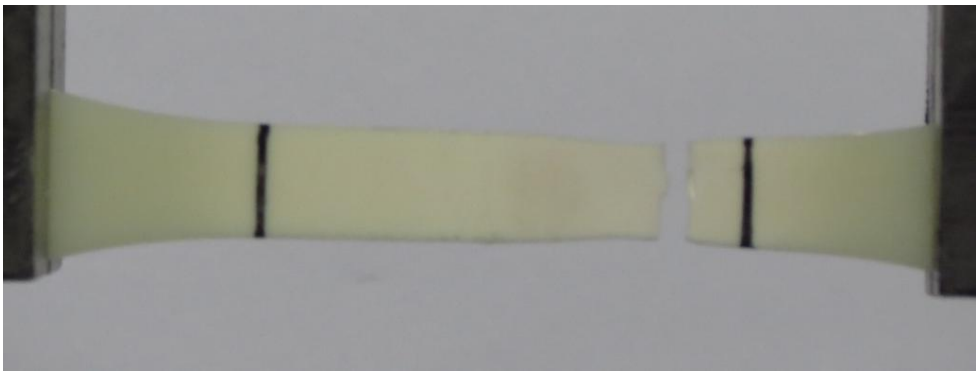

Figure 54. Bulk tensile XNR6852-1 specimen after the test.

4.2.2 Bulk tests at high temperature

The geometry and manufacturing process of the adhesive were the same as at room temperature. To perform the tests while the specimen was at 80 ºC a heating chamber specially designed for the INSTRON® universal test machine was used. Before assembling the specimen to the machine, the chamber was warmed up to the right temperature. A previous specimen with a thermocouple inside was tested to determine that in ten minutes the specimens could reach the temperature of 80 ºC (shown in Figure 55). The displacement was measured and recorded with the same system used for the RT tests.

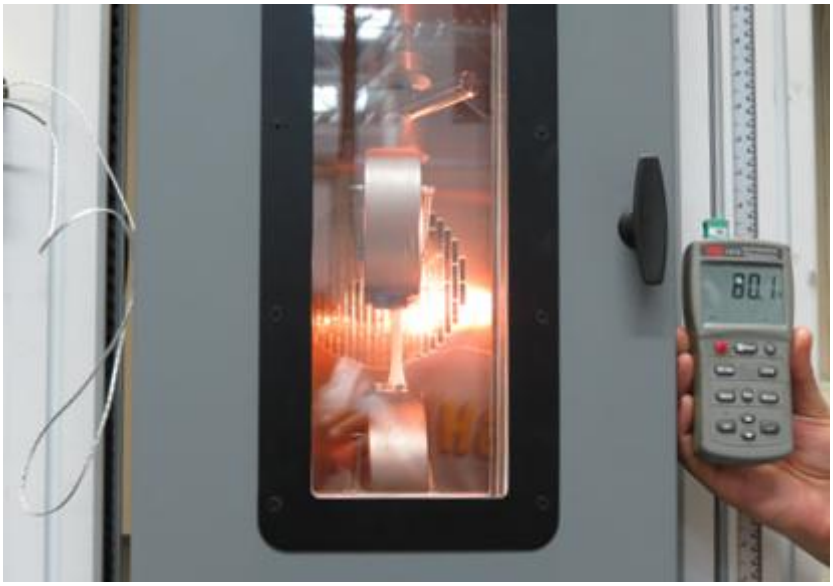

Figure 55. Checking of the temperature while testing the bulk specimens.

The first specimen tested showed a very high elongation comparing to the ones tested at RT, but it fractured near the grips while it should have broken in the necking region. For this reason, the following tests were stopped when the elastic part of the curve had been recorded. Although the strain value shown in Table 11 is not correct, it is safe to say that the ductility of the adhesive at 80 ºC is even higher.

Table 11. Mechanical properties of the adhesive at high temperature.

	Tensile strength (MPa)	Young's modulus (MPa)	Strain to failure (%)
XNR6852-1 80 ºC	10.88 ± 0.47	278.73 ± 2.41	100.9

A strong decrease in the mechanical properties of the adhesive can be observed, while the ductility increased in the same extent. The curve stress-strain obtained for the fractured specimen shows a typical behaviour from a thermoplastic polymer (see Figure 56). Different specimens are shown in Figure 57 with different strains. The fractured one deformed in a ductile manner in the entire specimen so that it almost broke by the end, where it was clamped.

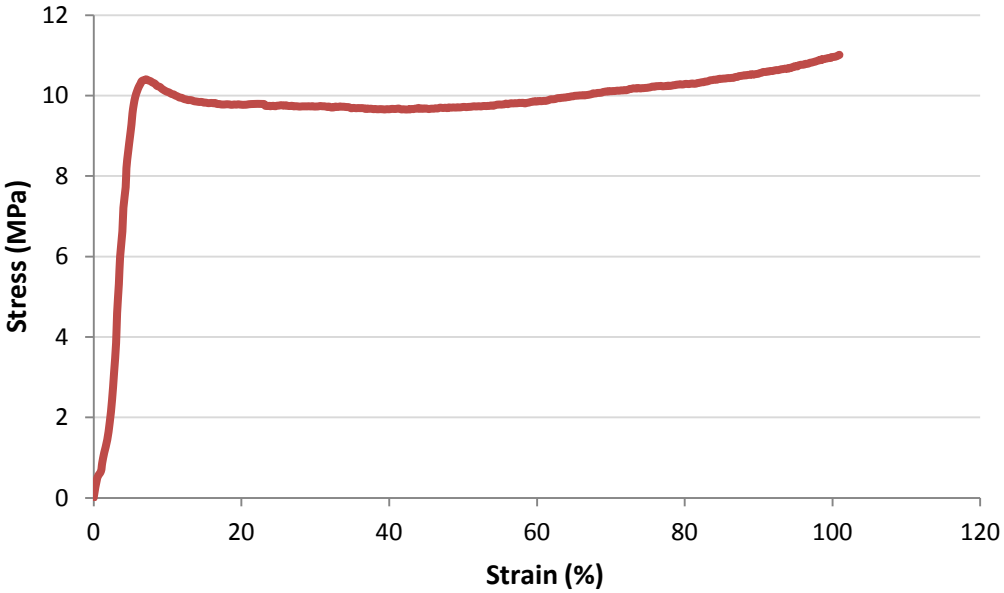

Figure 56. Stress-strain curve obtained from bulk tests at 80 ºC.

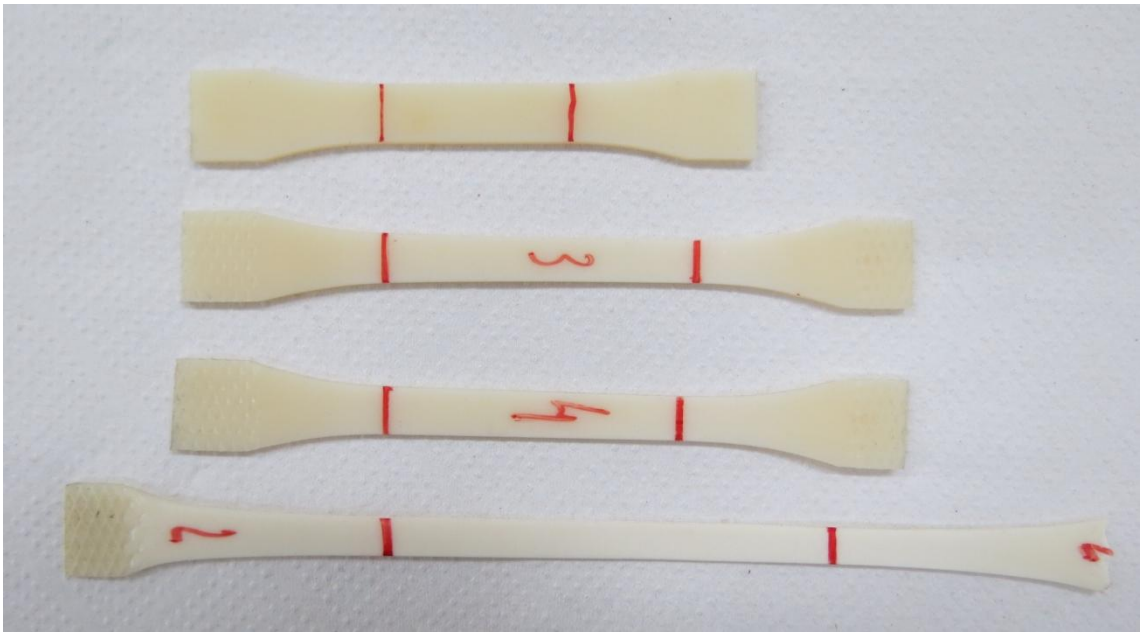

Figure 57. Bulk specimens tested until different strains at high temperature.

5. Analysis of results

5.1 Temperature and adhesive thickness influence on impact strength

A summary of the results obtained in the different impact tests is displayed in this section, showing the effect of temperature and adhesive thickness on different failure parameters. The results showed that the property most affected by the variation of temperature under high strain-rate was the capacity of absorbing energy (see Figure 58). In both cases at high and low temperatures, the mechanical properties of the adhesive were drastically reduced, causing the failure of the joint much sooner than at room temperature.

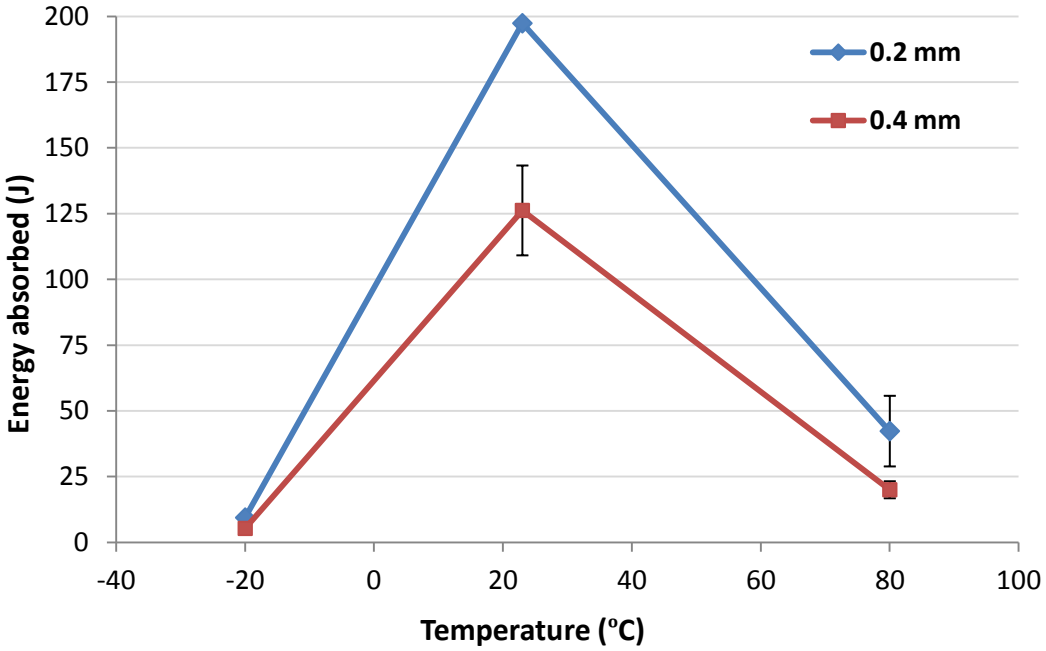

Figure 58. Energy absorbed vs. Temperature results for impact tests.

Regarding the results of maximum failure load as a function of temperature, it seemed that, although there was a decrease at high and low temperatures, the effect was not so significant (see Figure 59). Then, there seems to be a contradiction with these results and the ones obtained for the bulk tests at different temperatures, since the adhesive tensile strength suffered a strong variation when tested at 80 ºC. An explanation for this is given in the following section, where failure load prediction is done.

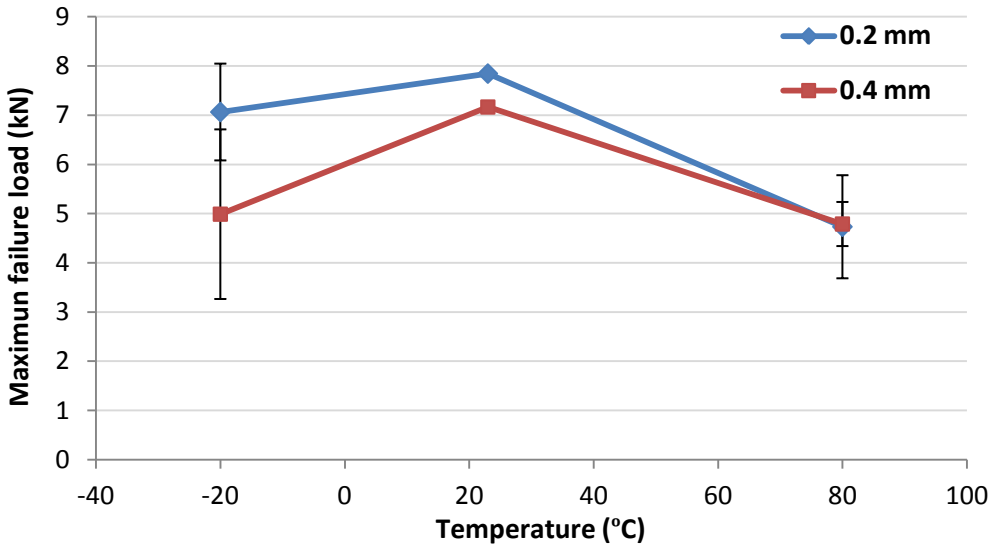

Figure 59. Max. failure load vs. temperature results for the impact tests.

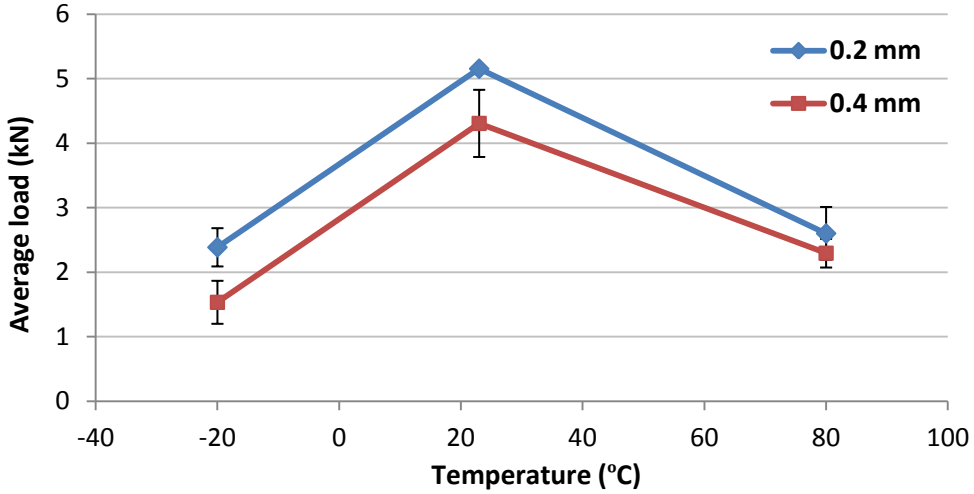

Figure 60. Average load vs. temperature results for impact tests.

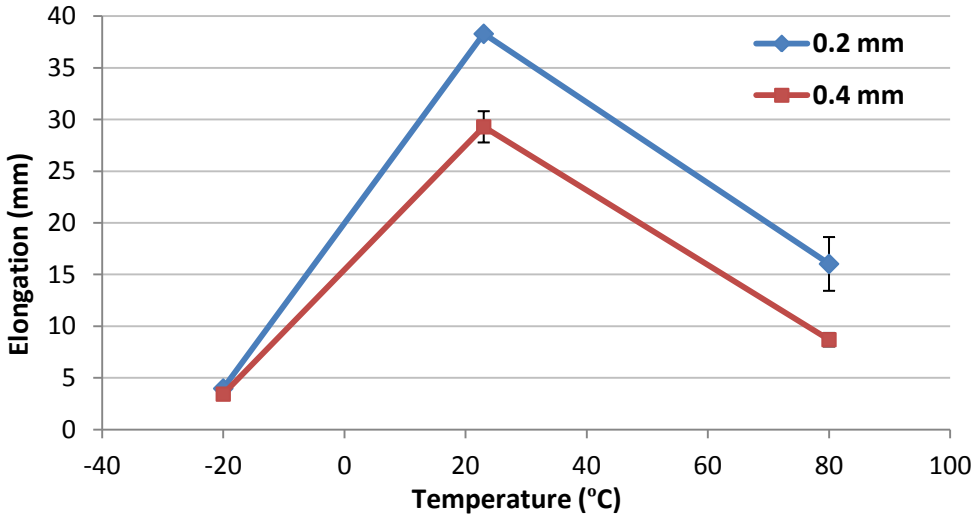

Figure 61. Elongation vs. temperature results for the impact tests.

Due to the high scattering of the data obtained for this parameter as a result of the vibration phenomena, an average load was calculated by dividing the energy absorbed by the elongation at fracture and is represented in Figure 60. Since the energy absorbed is obtained from the area below the load vs. elongation curve and load results were not highly influenced by temperature, it is expected for elongation to have a similar response as energy absorption as a function of temperature (see Figure 61).

The results as a function of the bondline thickness did not vary from the ones obtained under quasi-static load in previous studies. As explained in the literature review, the optimum value of adhesive thickness for an epoxy adhesive used in SLJs oscillates between 0.1 and 0.2 mm, since for higher values the bending moment increases the stress, reducing the joint strength. When tested under impact load, all the results for the SLJs with 0.4 mm bondline thickness were, as expected, lower than the 0.2 mm.

Since failure load and energy absorption are the two most characteristic parameters of impact testing, to conclude this section, Figure 62 summarizes all the results obtained as a function of these two parameters.

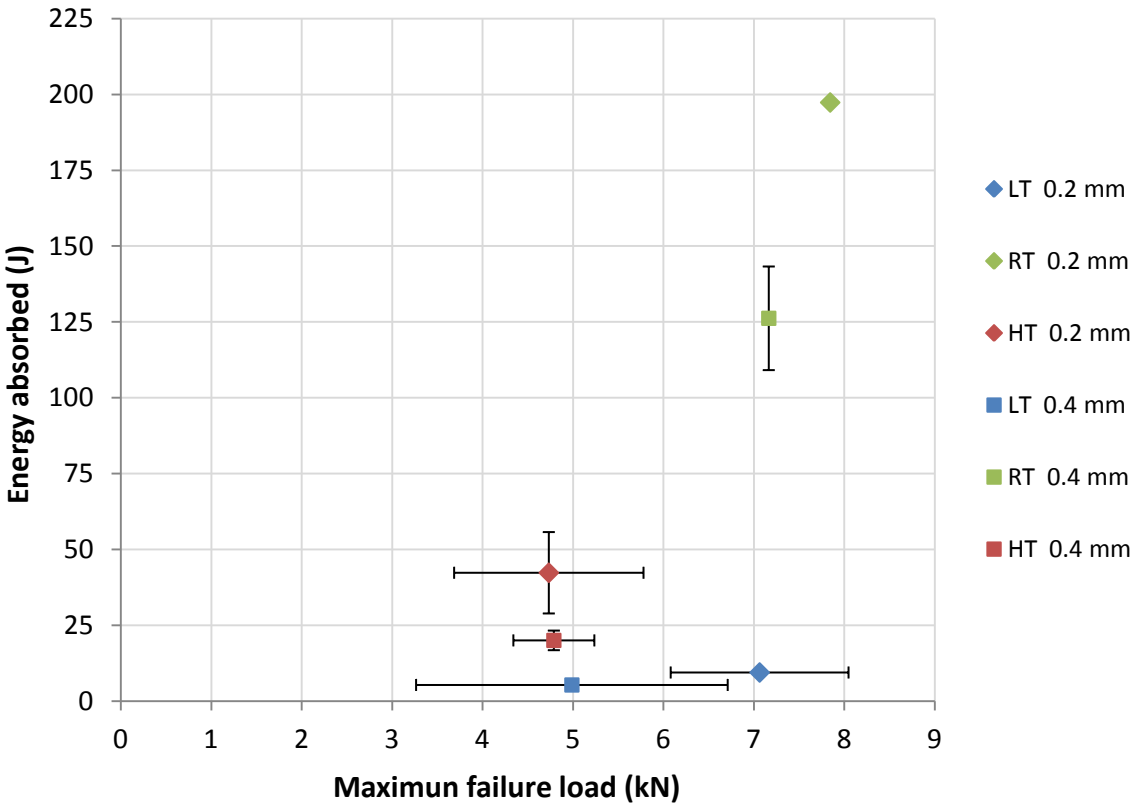

Figure 62. Energy absorbed vs. max. failure load results summary for the impact tests.

5.2 Failure load prediction

Now that the materials of the components of the SLJ have been characterized, the joint strength can be predicted by finding a suitable analysis model that explains the reasons of the failure. Although more complex models of analysis can be found in the literature, the Adams et al. [14] model was chosen to predict failure under impact load at room and high temperature. At room temperature the adherend yielding case is considered due to the high deformation observed in the substrates, while at high temperature the perceived adhesive weakness makes the global yielding a more suitable approximation.

Since it was not possible to obtain the properties of the adhesive at -20 ºC, no failure prediction could be done for low temperature impact tests. However, since the adhesive showed a brittle fracture surface at this temperature, the most suitable analysis to predict the joint strength would be the Volkersen's model [10].

5.2.1 Prediction at RT

In case of adherend yielding, Adams et al. [14] model explains the value of the failure load as a function of the tensile strength of the adherends material (10). As shown in the substrates characterization section, due to the high ductility of the steel used, the area reduced significantly while deformed. This also was observed in the adherends of the SLJs tested under impact at RT, as shown in Figure 30. For this reason, to calculate the predicted failure load both engineering and true tensile stresses were considered. Table 12 shows the predictions obtained compared with the experimental results at RT, where P_y and P_y* are the failure loads predicted using the engineering and the true tensile stresses, respectively.

Table 12. Experimental results vs. prediction of impact tests at room temperature.

Adhesive thickness	Max. failure load (kN)	Avg. failure load (kN)	Predicted - P_y (kN)	Predicted - P_y* (kN)
0.2 mm	7.85	5.15	4.87	6.29
0.4 mm	7.17 ± 0.04	4.31 ± 0.52		

Figure 63 represents graphically these results to have a more visual comparison between the curves predicted and the experimental results. The values for the prediction were obtained by interpolating the higher prediction value for long overlaps, when $k = 0$, and the lower prediction value for short overlaps, when $k = 1$ (see Figure 14).

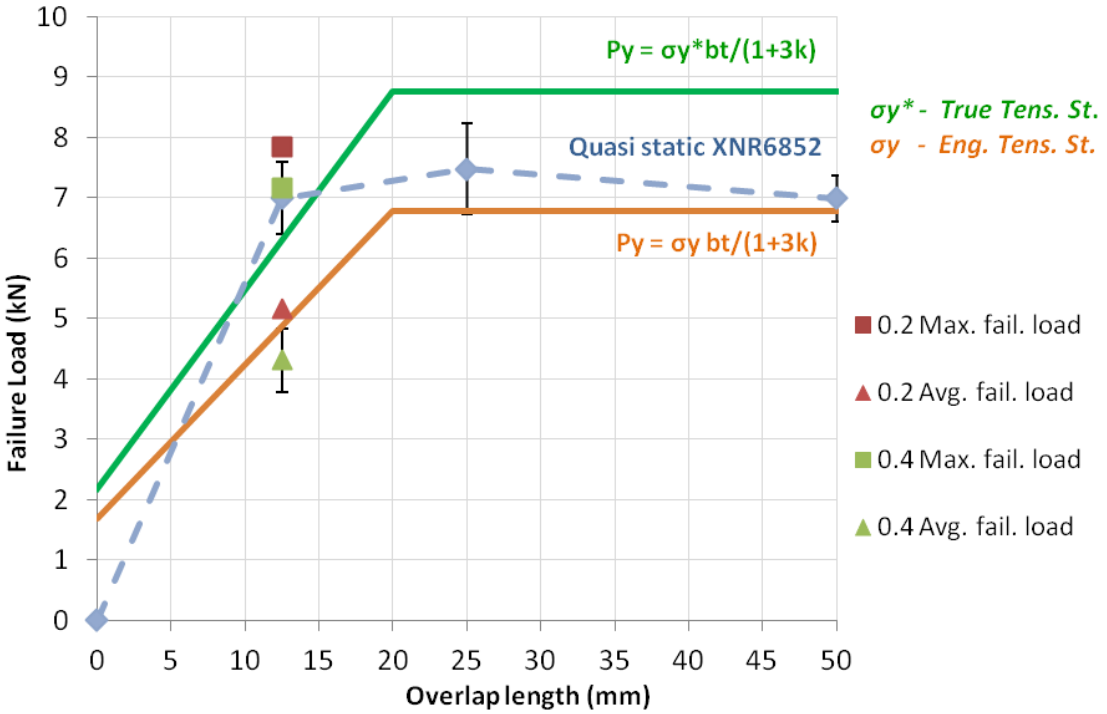

Figure 63. Adherend yielding prediction compared with experimental results at RT.

Results of quasi-static tests for the previous version of the adhesive as a function of the overlap length showed that the real curve gives higher value of failure load for an overlap of 12.5 mm, as shown in Figure 64 [23]. Consequently, it is normal that the values obtained by interpolating are slightly below the experimental values. Thus, it is expected that calculating the *k* factor by a more complex model of analysis will give more accurate predicted values.

In conclusion, when considering maximum failure load, the curve calculated with the true tensile strength of the steel seems to be a better approximation, while when average load is considered, the engineering tensile strength gives more similar predicted values. Since Adams et al. [14] model is used for quasi-static tests prediction, it is deduced that results obtained for the impact test can also be predicted with this model. The reason is that, the failure was mostly dictated by adherend yielding and the adherends are not very sensitive to strain rate, giving similar failure load values when tested under impact or quasi-static load.

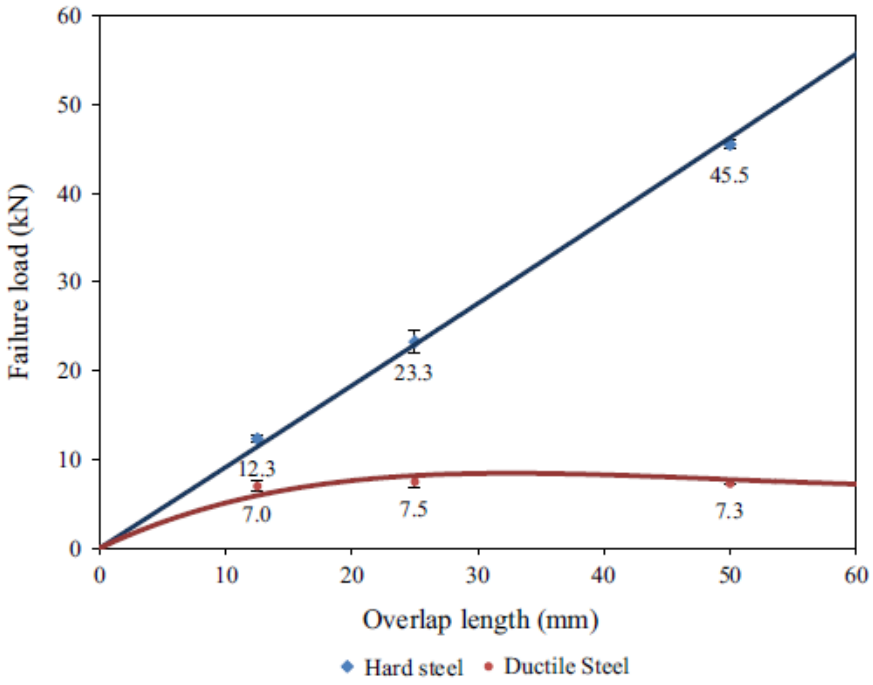

Figure 64. Results obtained for quasi-static tests with the previous version of the adhesive [23].

5.2.2 Prediction at 80 ºC

In this case almost no adherend yielding was perceived in the tested SLJs, and the fractured surface showed a ductile behaviour of the adhesive. Considering this, global yielding of the adhesive is the most suitable model of prediction for the impact tests at high temperature. The Adams et al. [14] global yielding model calculates the failure load P_a as a function of the shear strength of the adhesive (7). Supposing a von Misses yield model, the adhesive shear strength can be obtained as $\tau_y = \sigma_y/\sqrt{3}$. The results obtained at high temperature for the prediction compared with the experimental ones are summarized in Table 13 and represented graphically in Figure 65.

Table 13. Experimental and predicted results for impact strength at high temperature.

Adhesive thickness	Max. failure load (kN)	Avg. failure load (kN)	Predicted – P_a (kN)
0.2 mm	4.73 ± 1.05	2.6 ± 0.41	1.96
0.4 mm	4.79 ± 2.29	2.29 ± 0.45	

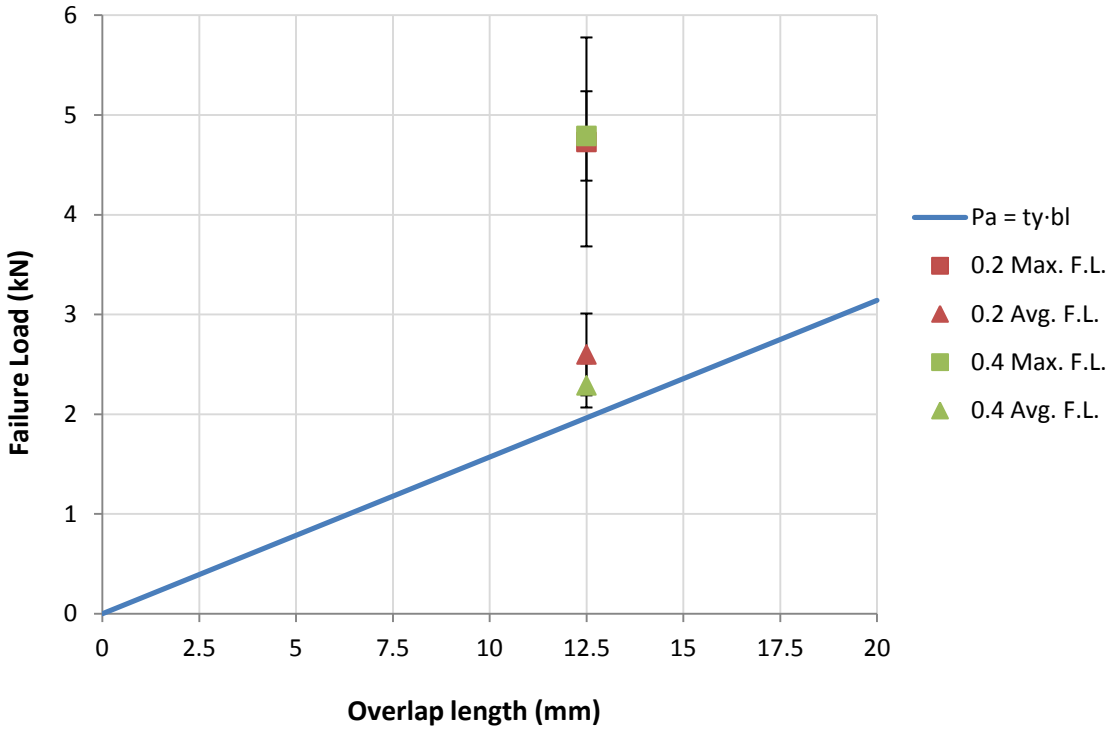

Figure 65. Global yielding prediction vs. experimental results at high temperature.

The prediction in this case is not as accurate as at room temperature, since the experimental values are much higher. The reason for this is that at high temperature the adhesive is the responsible of the joint failure, and it is much more sensitive at this temperature to the high strain-rate. Thus, unlike in room temperature prediction, the values of failure load expected for quasi-static tests at 80 ºC would be lower than when tested under impact load. Therefore, tests of the adhesive under high strain rate are necessary to have a good failure load prediction.

6. Conclusions

The heating and cooling systems implemented in the impact tests enabled successfully the characterization of the adhesive XNR6852-1 impact strength at -20, +23 and +80ºC.

At room temperature:

- The adhesive has high resistance under impact load, withstanding deformation and damage without brittle behaviour.
- Due to the high adherend yielding, the steel strength determines the failure of the SLJs.
- Tensile strength of the adhesive is high (approximately 60 MPa), typical of an epoxy adhesive.
- Less ductility (approximately 20% strain) is obtained for the adhesive, comparing with the previous version XNR6852 [23].
- Failure prediction using adherend yielding gives accurate values due to the low sensitivity of the steel to the strain-rate.

At high temperature:

- The resistance of the adhesive is strongly reduced, fracturing in a ductile manner before the steel adherends yield.
- Low tensile strength is obtained for the adhesive at 80 ºC (approximately 10 MPa).
- Ductility is highly increased for the adhesive (more than 100%), behaving as a thermoplastic polymer.
- The strong sensitivity of the adhesive to high strain-rate gives higher results for failure load than the prediction using static properties of the adhesive.

At low temperature:

- The adhesive shows low resistance under impact load as at high temperature.
- Typical brittle behaviour is observed in the fracture surface of the specimens.

7. Future work

Due to the wide range of possibilities available to study impact strength, some ideas are listed here to improve the results obtained and draw more conclusions:

- Obtain the adhesive properties at -20 ºC by performing bulk tests at this temperature.
- Perform the bulk tests of the adhesive with specimens with larger ends to prevent it from breaking near the grips.
- Determine the adhesive properties under high strain-rates.
- Conduct quasi-static tests at low and high temperatures of the SLJs and compare the results with the impact tests.
- Test under impact load SLJs with different overlap lengths to check if the tendency obtained is the same as for quasi-static tests.
- Analyze by FEA the impact strength in order to obtain more accurate predictions.

References

[1] L. F. M. da Silva, A. Öschner and R. D. Adams, Handbook of Adhesion Technology, 1 ed., Springer, 2011.

[2] W. A. Lees, Adhesives in Engineering Design, Springer Berlin Heidelberg, 1984.

[3] L. F. M. da Silva, A. G. de Magalhaes and M. F. S. F. de Moura, Juntas Adesivas Estruturais, 1 ed., 2010.

[4] S. R. Hartshorn, Structural Adhesives, Chemistry and Technology, Hartshorn, 1986.

[5] S. Ebnesajjad, Adhesives Technology Handbook, William Andrew, Elsevier, 2008.

[6] R. D. Adams, Adhesive Bonding, Science, Technology and Applications, Woodhead Publishing Limited, 2000.

[7] L. F. M. da Silva, P. J. C. das Neves, R. D. Adams and J. K. Spelt, "Analytical models of adhesively bonded joints - Part I: Literature survey," *Int. J. Adhesion Adhes.,* vol. 29, pp. 319-330, 2009.

[8] L. F. M. da Silva, P. J. C. das Neves, R. D. Adams and J. K. Spelt, "Analytical models of adhesively bonded joints—Part II: Comparative study," vol. 29, p. 331–341, 2009.

[9] R. D. Adams and J. Comyn, "Joining using adhesives," *Assembly Automation,* vol. 20, no. 2, pp. 109-117, 2000.

[10] O. Volkersen, "Luftfahrtforschung," vol. 15, 1938, pp. 41-47.

[11] M. Goland and E. Reissner, "The stresses in cemented joints," *J. Appl. Mech.,* vol. 11, pp. A-17 - A-27, 1944.

[12] L. J. Hart-Smith, "Adhesive-bonded Single-lap Joints," NASA contract report, 1973.

[13] X. L. Zhao, "Stress and failure analysis of adhesively bonded lap joints," 1991.

[14] R. D. Adams and W. C. Wake, Structural Adhesive Joints in Engineering, Elsevier Applied Science Publishers LTD, 1997.

[15] E. F. Karachalios, R. D. Adams and L. F. M. da Silva, "Single lap joints loaded in tension with ductile steel adherends," *Int. J. Adhesion Adhes.,* vol. 43, p. 96–108, 2013.

[16] L. D. R. Grant, R. D. Adams and L. F. M. da Silva, "Effect of the temperature on the strength of adhesively bonded single lap and T joints for the automotive industry," *Int. J.Adhesion*

Adhes., vol. 29, p. 535–542, 2009.

[17] L. D. R. Grant, R. D. Adams and L. F. M. da Silva, "Experimental and numerical analysis of single-lap joints for the automotive industry," *Int. J.Adhesion Adhes.,* vol. 29, p. 405–413, 2009.

[18] L. F. M. da Silva and R. D. Adams, "Stress-free temperature in a mixed-adhesive joint," *J. Adhesion Sci. Technol.,* vol. 20, pp. 1705-1726, 2006.

[19] R. D. Adams and V. Mallick, "The effect of temperature on the strength of adhesively-bonded composite-aluminum joints," *J. Adhesion,* vol. 43, pp. 17-33, 1993.

[20] L. F. M. da Silva and R. D. Adams, "Adhesive joints at high and low temperatures using similar and dissimilar adherends and dual adhesives," *Int. J. Adhesion Adhes.,* vol. 27, p. 216–226, 2007.

[21] A. Deb, I. Malvade, P. Biswas and J. Schroeder, "An experimental and analytical study of the mechanical behaviour of adhesively bonded joints for variable extension rates and temperatures," *Int. J. Adhesion Adhes.,* vol. 28, p. 1–15, 2008.

[22] J. F. P. Owens and P. Lee-Sullivan, "Stiffness behaviour due to fracture in adhesively bonded composite-to aluminum joints, part 2: experimental," *Int. J. Adhesion Adhes.,* vol. 20, p. 47–58, 2000.

[23] D. F. S. Saldanha, C. M. S. Canto, L. F. M. da Silva, R. J. C. Carbas, F. J. P. Chaves, K. Nomura and T. Ueda, "Mechanical characterization of a high elongation and high toughness epoxy adhesive," *Int. J. Adhesion Adhes.,* vol. 47, p. 91–98, 2013.

[24] J. A. Harris and R. D. Adams, "An Assessment of the Impact Performance of Bonded Joints for Use in High Energy Absorbing Structures," *J. Mech. Eng. Science,* vol. 199, pp. 121-131, 1985.

[25] L. F. M. da Silva, D. A. Dillard, B. R. K. Blackman and R. D. Adams, Testing Adhesive Joints, Best Practices, John Wiley & Sons, 2012.

[26] R. D. Adams and J. A. Harris, "A critical assessment of the block impact test for measuring the impact strength of adhesive bonds," *Int. J. Adhesion Adhes.,* vol. 16, p. 61–71, 1996.

[27] B. R. K. Blackman, A. J. Kinloch and A. C. Taylor, "The impact wedge-peel performance of structural adhesives," *Journal of Materials Science,* vol. 35, pp. 1867-1884.

[28] H. Kolsky, "Stress Waves in Solids," *J. Sound Vibration,* vol. 1, p. 88–110, 1964.

[29] H. Zhao, G. Gary and J. R. Klepaczko, "On the use of a Viscoelastic Split Hopkinson Pressure Bar," *Int J Impact Eng,* vol. 19, p. 319–330, 1997.

[30] C. M. S. Canto, “Strength and fracture energy of adhesives for the automotive industry,” Master thesis in FEUP (Universidade do Porto), 2013.

[31] V. Rudnev, D. Loveless, R. L. Cook and M. Black, Handbook of Induction Heating, CRC Press, 2014.

[32] R. J. C. Carbas, L. F. M. da Silva and G. W. Critchlow, “Adhesively bonded functionally graded joints by induction heating,” *Int. J. Adhesion Adhes.,* vol. 48, p. 110–118, 2014.

[33] G. N. Gonzalez, “Aplicaciones del calentamiento por inducción electromagnética en el procesamiento de PRFV,” PRFV/Composites, 2005.

[34] “Petrieltd,” 7 6 2014. [Online]. Available: www.petrieltd.com/index.php/Induction.

[35] W. Gonzalez, “Diseño y construccion de bobina de calentamiento por inducción para fundición de titanio,” Graduate thesis, Universidad Simón Bolívar, 2008.

[36] D. Roylance, “Stress-strain curves,” Departament of Materials Science and Engineering, MIT, Cambridge, MA, 2001.